12-2021

Tracking Vibrio: Population Dynamics and Community Ecology in Alabama Estuaries

Blair H. Morrison
University of Alabama, bmorrison@disl.org

TRACKING VIBRIO: POPULATION DYNAMICS AND COMMUNITY ECOLOGY IN ALABAMA ESTUARIES

A Thesis

Submitted to the Graduate Faculty of the
University of South Alabama
in partial fulfillment of the
requirements for the degree of

Master of Science

in

Marine Sciences

by
Blair H. Morrison
B.S., The University of Alabama, 2018
December 2021

For my family, both near and far.

ACKNOWLEDGEMENTS

"It was the best of times, it was the worst of times, it was the age of wisdom, it was the age of foolishness, it was the epoch of belief, it was the epoch of incredulity, it was the season of light, it was the season of darkness…"

It's no secret that grad school isn't easy. Add in the death of a grandparent, a global pandemic, an unprecedented hurricane season, and a destroyed apartment and it's downright difficult. But it's made easier when you have an amazing support system, fantastic collaborators, and friends who are now family. Thanking all the amazing people who have helped me along the way is the least I can do.

I would first like to thank my committee for their enthusiasm, patience, adaptability, and investment in me as a young scientist. I would also like to thank Jeremiah Henning for sharing his stats knowledge with me. The FDA/DISL Fellowship program supported my research and gave me the opportunity to make connections with federal, state, and academic partners – opportunities that I am truly grateful for.

I would like to thank Joie Horn and Clark Gerken at ADEM, Drew Sheehan and the staff of the ADPH Phytoplankton Lab, Glen Chaplin, Scott Rikard, Vicki Pruente, James Kelly, and the staff of AUSL, Keri Lydon, Madison McGough, Joey Marchant, Whitney

Neil, and the personnel of the GCSL. This project would not have been possible without your generosity and willingness to help.

To the PhySSi Lab- your support, laughter, companionship, and enthusiasm for decorating has made my experience infinitely more meaningful. Thank you to Rebecca Pickering, Alex Marquez, Kyle Halstead, Cassie Bates, Randi Cannon, and Allie Smith (who has assured me that she will take over as head Gremlob for the lab).

To the DISL Graduate Student Community: thank you all for your support, camaraderie, beach happy hours, and Mardi Gras memories.

To Edward Kim- thank you for being the best roommate ever and putting up with my shenanigans (and hatred of dishes). And thank you to Lauren Clance and Kara Gadeken for joining in our tomfoolery.

Last but not least, thank you to my family, for believing in me even when I didn't.

TABLE OF CONTENTS

Page

LIST OF TABLES

LIST OF FIGURES

LIST OF ABBREVIATIONS

Abbreviation	Meaning
ADEM	Alabama Department of Environmental Management
ADPH	Alabama Department of Public Health
APW	Alkaline Peptone Water
ARCOS	Alabama Real Time Coastal Observing System
BHQ1/BHQ2	Black Hole Quencher 1 / 2
CDC	Center for Disease Control and Prevention
CFSAN	Center for Food Safety and Applied Nutrition
Cy5	fluorescent cyanine dye
DI	Dauphin Island
DISL	Dauphin Island Sea Lab
DRP	Dissolved Reactive Phosphorus
EMSS	Eastern Mississippi Sound System
FDA	Food and Drug Administration
FAO	Food and Agriculture Organization
GCSL	Gulf Coast Seafood Lab
GOM	Gulf of Mexico
HAB	Harmful Algal Bloom

IAC..... Internal Amplification Control

JOE.....2′,7′-dimethoxy-4′,5′-dichloro-6-carboxyfluorescein

LME .....Linear Mixed Effects Model

LOD .....Limit of Detection

MPN..... Most Probable Number

NH_3..... ammonia

NMDS.....Non-Metric Dimensional Scaling

NOAA.....National Oceanographic and Atmospheric Administration

NO_x.....nitrate/nitrite

NTU ..... Nephelometric Turbidity Unit

PAR..... Photosynthetically Active Radiation

PBS.....Phosphate Buffered Saline

PCR..... Polymerase Chain Reaction

PERMANOVA .....Permutational Multivariate Analysis of Variance

TCBS .....Thiosulfate-Citrate-Bile Salts-Sucrose

tlh ..... thermolabile hemolysin

TSS.....Total Suspended Solids

USGS ..... United States Geological Survey

Vp..... *Vibrio parahaemolyticus*

Vv..... *Vibrio vulnificus*

vvh .....vibrio vulnificus hemolysin

WHO.....World Health Organization

ABSTRACT

Morrison, Blair H., M. S., University of South Alabama, December 2021. Tracking *Vibrio*: Population Dynamics and Community Ecology in Alabama Estuaries. Chair of Committee: Jeffrey W. Krause, Ph.D.

Integral parts of local culture along the Eastern Mississippi Sound System (EMSS)- eating raw oysters and fishing- can involve contact with vectors of pathogenic *Vibrio* spp. bacteria. High mortality rates from vibrio infections demonstrate the need for improved understanding of *V. vulnificus* and *V. parahaemolyticus* dynamics in the region. This study assessed: 1) meteorological, 2) hydrographic, and 3) biological correlates of *V. parahaemolyticus* and *V. vulnificus* in the EMSS from April-October 2019. Spearman's correlations, linear mixed models, and non-metric dimensional scaling identified significant relationships between *Vibrio* spp., abiotic, and biotic parameters of the ecosystem. *Vibrio* spp. population dynamics were largely driven by site-based variation, with sites closest to freshwater inputs having the highest *Vibrio* spp. abundances. These data also suggest that the E-W wind scalar may be a novel *Vibrio* spp. correlate in the EMSS, and there may be a salinity effect on *V. vulnificus*-particle associations. Additionally, *V. vulnificus* abundances were correlated to harmful algal species like *Akashiwo sanguinea* and *Heterocapsa* spp. Correlates from this study can be used to inform the next iteration of predictive *Vibrio* models for the EMSS region.

CHAPTER 1 INTRODUCTION

The lifestyle of the Alabama Gulf Coast community is intrinsically linked to the waters of Mobile Bay, Mississippi Sound, and the northern Gulf of Mexico. Unfortunately, integral parts of this culture - eating raw oysters (*Crassostrea virginica*), fishing, and recreational water sports- can also involve contact with potential vectors of *Vibrio* spp. bacteria. *Vibrio* is a genus of halophilic, gram-negative bacteria that can be found in estuaries around the globe. The genus contains several known human pathogenic species including *V. parahaemolyticus*, *V. vulnificus*, *V. cholerae*, *V. alginolyticus, V. mimicus, V. fluvialis, V. furnissii, V. metschnikovii,* and *V. hollisae* (Pruzzo et al. 2005). The Center for Disease Control and Prevention estimates that over 80,000 cases of vibrio related illness occur each year (CDC 2018), with raw oyster consumption being largely responsible for enteric cases of *Vibrio* spp. infection (vibriosis) in the United States. While many individuals recover fully from vibriosis within days, 25% of those infected by *V. vulnificus* die from exposure to the bacterium (CDC 2018). High rates of morbidity and mortality demonstrate the need for improved understanding, and ultimately prediction, of *V. vulnificus* and *V. parahaemolyticus* population dynamics in coastal regions where they occur in proximity to human activities.

The Eastern Mississippi Sound System (EMSS) is a spatially and temporally dynamic estuary including the western portion of Mobile Bay, coastal embayments

(Cedar Point, Grand Bay, Portersville Bay, Fowl River Bay), the eastern Mississippi Sound, and two barrier islands (Dauphin Island and Petit Bois). Varying freshwater input and meteorological forcing conditions create complex biophysical gradients which affect biological communities in the system (Du et al. 2018, Kim and Park 2012, Kim et al. 2013, Lehrter et al. 1999, MacIntyre et al. 2011). Therefore, it is important to assess the connectivity between fluvial input, fluvially influenced hydrographic parameters, and *Vibrio* spp. populations in the EMSS. Past studies have shown that *V. vulnificus* and *V. parahaemolyticus* abundances are typically correlated to simple hydrographic metrics, e.g., temperature and salinity (Davis et al. 2019). Both vibrio species grow best when water temperatures are warm (≥20°C; Percival and Williams 2014); *V. vulnificus* tends to have lower optimal salinities than *V. parahaemolyticus* (Table 1). However, relative importance of these parameters varies considerably across regional and temporal scales (Takemura et al. 2014). This study offers the opportunity to identify and refine correlative parameters, particularly in relation to effects of fluvial input —which dominates the local hydrography. Fluvial input is most often accompanied with a diagnostic suite of hydrographic fluxes: decreases in salinity and pH and increases in turbidity (lowering irradiance) (Boesch et al. 2000). Freshwater discharge also affects concentrations of bio-limiting nutrients (nitrogen, phosphorus, silicic acid) and alters physical stratification of the water column (Boesch et al. 2000, Dzwonkowski et al. 2011, 2018). Geographic extent of freshwater influence in the EMSS is also subject to alteration from wind events along or across the estuary (Coogan and Dzwonkowski 2018). Given that Mobile Bay drains nearly all of the state of Alabama, and the watershed discharges over 50 billion cubic meters of water annually (Mobile Bay National Estuary Program

2019), we expect to see correlations between vibrio abundances and fluvial discharge into the EMSS.

Table 1. Optimal salinities for *Vibrio vulnificus* and *Vibrio parahaemolyticus*.

Note: The vibrio species targeted in this study prefer alkaline pH conditions (Chart 2012)		($7.0 < pH_{vibrio} < 9.0$)
Species	Optimal Salinity (S)	Source
Vibrio vulnificus	5 ppt < S < 10 ppt	Randa et al. 2004
Vibrio vulnificus	10 ppt < S < 20 ppt	Givens et al. 2014
Vibrio vulnificus	S ~ 15 ppt	Lipp et al. 2001
Vibrio vulnificus	7 ppt < S < 16 ppt	Kelly 1982
Vibrio vulnificus	5 ppt < S < 25 ppt	Motes et al. 1998
Vibrio parahaemolyticus	10 ppt < S < 20 ppt	Givens et al. 2014
Vibrio parahaemolyticus	S ~ 17 ppt	DePaola et al. 2003
Vibrio parahaemolyticus	15 ppt < S < 25 ppt	Givens et al. 2014

Kim and Park (2012) have shown that under the typical micro-tidal regime of Mobile Bay (not accounting for wind or excessive river discharge), most fresh water draining from the Mobile-Tensaw Delta exits Mobile Bay through the Main Pass, but anywhere from 25-33% fluxes through Pass-aux-Herons into the EMSS. Under northeast wind conditions, however, water fluxing out of Mobile Bay can be disproportionately funneled through Pass-aux-Herons rather than Main Pass, which has implications for salinity and flow regimes. Overall, salt is gained in the estuary through Main Pass and lost at a nearly equivalent rate through Pass-aux-Herons (Kim and Park 2012; Lee et al. 2019). Nonetheless, large freshwater discharge plume can still exit through the Main Pass, which may be acted upon by Coriolis effect, steering it to the right (westward flowing) and entraining into coastal currents (Dzwonkowski et al. 2015, Gelfenbaum and Stumpf 1993).

Higher rates of fluvial input correlate to greater turbidity in coastal waters, which has been shown to positively affect *Vibrio* spp. abundances (Johnson et al. 2010; Zimmerman et al. 2007). Therefore, spikes in *Vibrio* spp. abundances are expected to correlate with high turbidity events. Resuspension of sediments can also inject nutrients (both dissolved inorganic and organic forms) into the water column while diminishing the euphotic zone depth; heterotrophic bacteria, like vibrios, can use these resources at the expense of phytoplankton which require light. This expected correlation would be limited by salinity tolerances for vibrio species (Table 1).

Along with the effects of fluvial input, we wish to evaluate potential *Vibrio* spp. correlations with the planktonic community. It has been observed that many species of bacteria (including several in the *Vibrio* genus) have associations with detritus and planktonic organisms because the bacteria can use them as a growth "substrate" (Gilbert et al. 2012, Harriague et al. 2008, Huq et al. 1983, Main et al. 2015, Montanari et al. 1999, Takamura et al. 2014, Turner et al. 2009). *Vibrio* spp. have been also shown to readily associate specifically with chitinous organisms (Figure 1) and phytoplankton aggregates (Harriague et al. 2008; Montanari et al. 1999; Turner et al. 2009). Although vibrio-plankton associations have been investigated in other estuary systems, these relationships have not been studied in Mobile Bay or Mississippi Sound. Vibrio-particle size relationships remain to be elucidated in the EMSS as well.

Vibrio spp. may also live in close association to various phytoplankton species to take advantage of "phycospheres", small regions of concentrated organic carbon sources created by phytoplankton cellular exudates (Bell and Mitchell 1972; Moran 2015). This association may be particularly strong with harmful bloom-forming dinoflagellate species

(Greenfield et al. 2017; Takemura et al. 2014), several of which have been documented in Mobile Bay over the past two decades (Table 3). In other estuary systems, ties between phytoplankton and vibrios were so tightly coupled that DeMagny et al. (2008) used lagged chlorophyll a anomalies to predict abundances of *Vibrio cholerae*; however, this trend may not be universal (Rehnstam-Holm et al. 2010). According to Holiday's dissertation (2009), salinity, dissolved organic phosphorus, and dissolved organic nitrogen are the most important structuring factors to the phytoplankton community of Mississippi Sound and Mobile Bay. Therefore, within the photic zone, we hypothesize that *Vibrio* spp. will co-occur with phytoplankton communities which share overlapping hydrographic requirements (salinity, temperature, nutrients). This study offers an opportunity to further evaluate the efficacy of using phytoplankton to predict increased abundances of vibrio species in Mobile Bay.

Table 2. Summary table of common harmful algal bloom (HAB) species reported in Mobile Bay and the Mississippi Sound.

Phytoplankton Type	Genus/ Species name	Source
Diatoms	*Pseudo-nitzschia* spp.	Holiday et al. 2007
Dinoflagellates	*Karenia brevis; Gymnodinium sanguineum; Dinophysis caudata; Prorocentrum minimum; Karenia mikimotoi*	Landsberg 2002
Dinoflagellates	*Karlodinium veneficum; Heterocapsa triquetra; Akashiwo sanguinea*	Holiday 2009
Dinoflagellates	*Gonyaulax spinifera; Gonyaulax polygramma*	Steidinger & Penta 1999

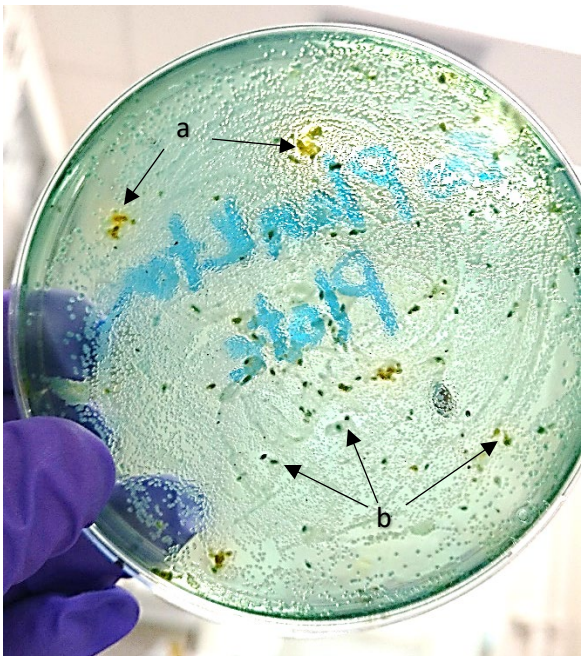

Figure 1. Bacterial colonies associated with the surfaces of copepods and other chitinous planktonic organisms. A zooplankton sample (63 µm mesh) collected along the 20-m isobath south of Dauphin Island was plated directly onto Thiosulfate-Citrate-Bile-salts-Sucrose (TCBS) agar. After 24 hours of incubation, the plate yielded both sucrose metabolizing (a) yellow and non-sucrose metabolizing (b) green colonies associated with the external surfaces of apparent copepods and other organisms. Due to the selective qualities of the media, these colonies are likely *Vibrio* spp., but were not genetically confirmed.

Although *Vibrio* spp. dynamics in the EMSS are an important issue for public health, many data gaps exist. Previous Food and Drug Administration (FDA) /Dauphin Island Sea Lab (DISL) partnership work has examined temporal dynamics of *V. cholerae* abundances in the water column, sediments, and oysters (Nash 2018), but there is still much unknown about population dynamics of other *Vibrio* spp. in the water column, especially in conjunction with freshwater input. This study aims to better assess: 1) meteorological, 2) hydrographic, and 3) biological correlates of *Vibrio parahaemolyticus* (Vp) and *Vibrio*

vulnificus (Vv) in the fluvially- driven EMSS to improve future modelling and mitigation of public health risks. Due to the integrative scope of this study, hydrographic and meteorological data from this project may offer greater resolution in forecasting for NOAA and FDA predictive models, while identified biological relationships with *Vibrio* spp. may enable local monitoring programs [ADPH, Alabama Department of Environmental Management (ADEM)] to leverage their collective sampling data. Synergy between models, federal partners, and state agencies can then be relayed to stakeholders most readily affected by vibrio risk (oyster farmers, commercial fishermen, etc.).

CHAPTER 2 METHODS

2.1 Sampling Sites

This study was conducted in EMSS and coastal Alabama, both under the hydrographic influence of Mobile Bay to the east (Figure 2). Sampling was done in conjunction with the Alabama Department of Environmental Management (ADEM) water quality monitoring field team, the chosen sites in this region are used by the ADEM every three years for routine monitoring. These study sites include coastal bays (Fowl River Bay, Grand Bay, Portersville Bay- FRB, GB-1, GB-2, and PB), a central sound (Mississippi Sound and Western Mobile Bay – MS-1, MS-2, and MB-1A), and barrier island localities (Pelican Island, Petit Bois Pass and Gulf of Mexico sites – PEIM, GOM-1, and GOM-2). This region has a micro-tidal regime (Schroeder et al. 1999) and is freshwater dominated; thus, the sites were expected to display fluctuations in salinity throughout the year due to freshwater input.

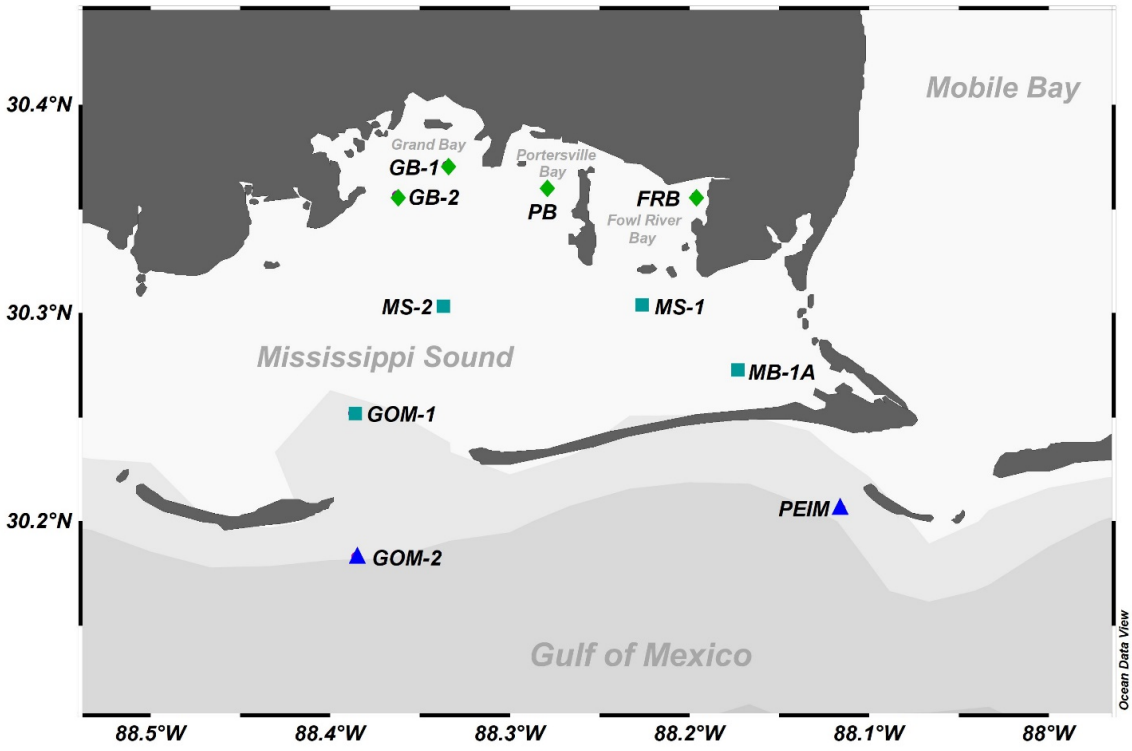

Figure 2. Sampling sites in the Mobile Bay/Mississippi Sound System. Symbols represent Alabama Department of Environmental Management (ADEM) water quality monitoring sites, sampled monthly from April-October 2019. These sites are roughly grouped into three sections: coastal bays (green symbols), sound (teal symbols), and barrier island (dark blue symbols). Map created using Ocean Data View software (Schlitzer 2021)

2.2 Meteorological Data

Wind speed, wind direction, and precipitation for 2019 were recorded by the Alabama Real-time Coastal Observing System (ARCOS) Meteorological Station on Dauphin Island (DI). ARCOS stations closer to sampling points in the EMSS were considered, but trends in wind speed and direction at these sites were highly correlated to the Dauphin Island station ($r > 0.69$, r-critical = 0.17 at $\alpha = 0.01$) and the DI station had the most consistent data quality for 2019. Archived data was accessed from the ARCOS website (https://arcos.disl.org/). Wind direction measurements were recorded at a height of 10 m and reported in standard meteorological notation (i.e., direction notates the origin of the wind, not the direction it is going) with 360°/0° signifying North. Wind speed and direction were transformed into scalar components (N-S and E-W vectors) via trigonometric calculations (Figure 3) (e.g., Krause et al. 2020). Tidally filtered river discharge data for the Mobile River (a key tributary to the Mobile -Tensaw Delta) was collected by the United States Geological Survey river gauge station #02470629 in Bucks, AL. Archived data was accessed from the USGS website (https://waterdata.usgs.gov/nwis/uv?site_no=02470629). Precipitation recorded by the ARCOS station was used as a proxy for local freshwater input via precipitation, whereas freshwater input from upstream precipitation was captured by river discharge data.

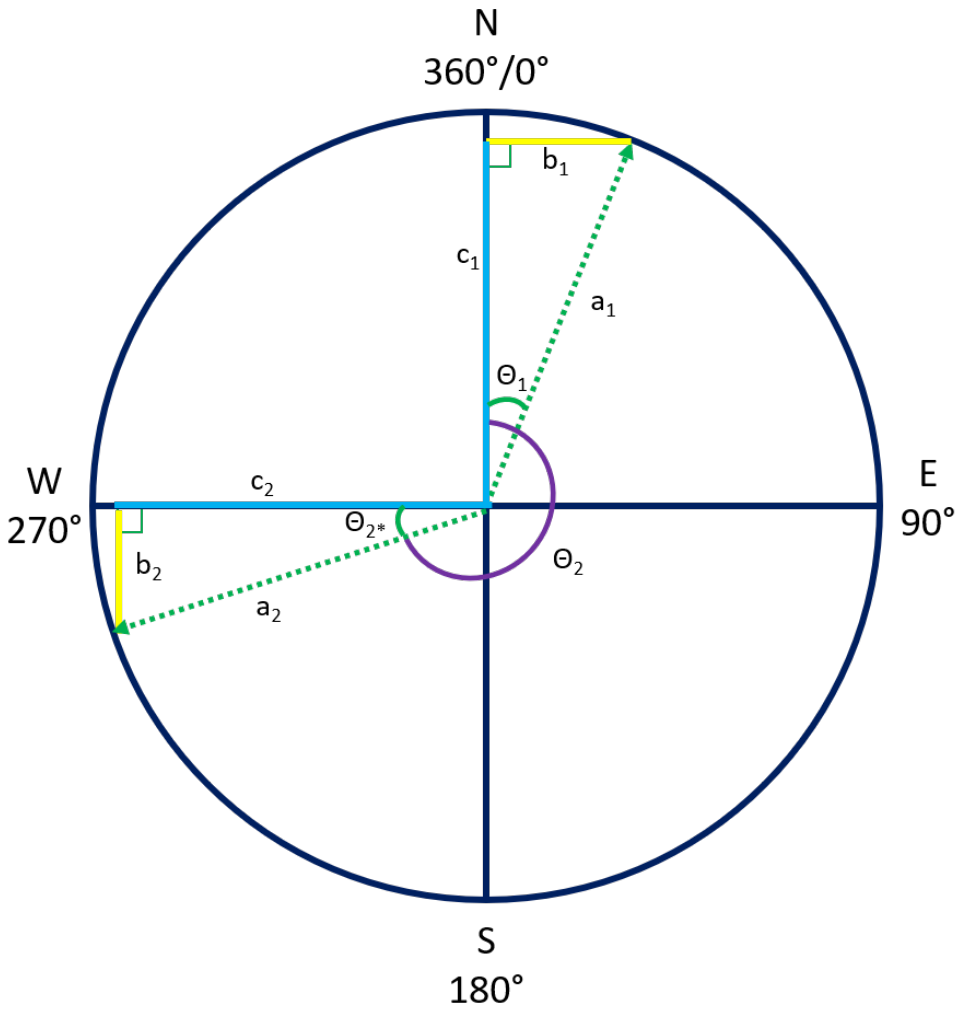

Figure 3. Examples of transforming wind direction and speed into scalar components. Θ represents the angle of wind direction and the variable 'a' represents the wind speed, as recorded by the ARCOS meteorological station. In Example 1 (indicated via subscript 1), the E-W wind scalar (b_1) is calculated by multiplying the wind speed (a_1) by the sine of the wind direction angle (Θ_1). The N-S wind scalar (c_1) is calculated by multiplying the wind speed (a_1) by the cosine of the wind direction angle (Θ_1). In Example 2 (indicated via subscript 2), the angle of the wind direction (Θ_2) is obtuse; therefore, the wind angle is subtracted from the nearest 90° increment (for this example, 270°) to get an acute angle (Θ_{2*}). The E-W wind scalar (c_2) is calculated by multiplying the wind speed (a_2) by the cosine of the transformed wind direction angle (Θ_{2*}). The N-S wind scalar is calculated by multiplying the wind speed (a_2) by the sine of the transformed wind direction angle (Θ_{2*}). The N-S scalar would be positive in Example 1 (originating from the north - c_1) and negative in Example 2 (originating from the south – b_2). The E-W scalar would be positive in Example 1 (originating from the east - b_1) and negative in Example 2 (originating from the west – c_2)

2.3 Field Sampling

Water samples for *Vibrio* spp. enumeration were collected at each site once a month from April – October 2019. Upon arriving at a site, the euphotic zone depth was determined using an LI-400 handheld photosynthetically active radiation (PAR) meter outfitted with an LI-192 underwater quantum sensor (LiCor Biosciences, Lincoln, NE). The base of the euphotic zone was defined as the depth where less than 1% of ambient surface PAR was detected by the submersible sensor. Hydrographic data, e.g., water temperature, conductivity (salinity), pressure (depth), and total dissolved solids were recorded using a YSI EXO 2 data sonde (YSI/Xylem Inc, Yellow Springs, OH) in full depth profiles with an approximate depth resolution between 0.5-1 meters. Once the base of the euphotic zone was determined, depth-integrated euphotic zone samples were collected using a sump pump (3028 liters/hour) attached to a hose that was raised and lowered through the water column at an approximate rate of one meter every 5 seconds. Two 4-L replicate water samples were collected at each site and stored in polypropylene bottles. An additional 1-L depth-integrated sample was collected from the euphotic zone at each site for phytoplankton analysis. Each phytoplankton sample was stored in a 1L glass jar and preserved using 7 mL of 12% Lugol's iodine solution. Hydrographic parameters and nutrients including nitrate, nitrite, chlorophyll a, phosphate, ammonia, alkalinity, total suspended solids, and turbidity were assessed in accordance with ADEM standard operating procedures (Alabama Department of Environmental Management 2016). All sampling was conducted within a 3-hour window of 07:00 local time. Water samples for *Vibrio* spp. enumeration were placed in a cooler, transported to the FDA Gulf Coast Seafood Lab within 40 minutes of returning to the dock, and were processed on the

same day. Hydrographic and nutrient samples collected by ADEM, were transported on ice, and delivered to the ADEM Chemistry and Microbiology Lab (Mobile, AL).

2.4 Preparation of Samples for *Vibrio* spp. analysis

Samples were processed using sequential filtration to fractionate the planktonic community based on size. Duplicate 100 mL aliquots from each sample were sequentially filtered through 35-micron Nitex mesh (CellMicroSieve, BioDesign Inc of New York, Carmel, NY) and then a 5-micron polycarbonate membrane (47mm diameter hydrophilic, Isopore, Darmstadt, Germany), with particles smaller than 5 microns being pelleted via centrifugation (10 min at 5000 x *g*). Each filter and pellet were resuspended via vortexing for 1 min in 10 mL of Phosphate Buffered Saline (PBS; 0.765% NaCl, 0.0724% Na_2HPO_4, 0.021% KH_2PO_4, pH 7.4 ± 0.2) and used as inoculum for Most Probable Number (MPN) – Real-time PCR analysis (Kaysner and DePaola 2004; Kinsey et al. 2015). MPN series were created by inoculating triplicate alkaline peptone water (APW; 1% BactoPeptone, 1% NaCl, pH 8.5 ± 0.2) tubes with 1 mL of the resuspended sample, followed by serially diluting each resuspended sample 1:10 with PBS through a 10^{-5} dilution and then transferring 1 mL of the serial dilutions into triplicate alkaline peptone water tubes (Figure 4). Following inoculation, each MPN series was incubated at 35± 2°C for 18-24 hours. Subsamples of APW with positive growth (turbidity) after incubation were boiled on a heat block at 97-100 °C for 10 minutes to create DNA lysates. Lysates were stored at -20°C until used in real-time PCR; all thawed lysates were centrifuged at 10,000 x *g* for 2 min before using as templates for real-time PCR.

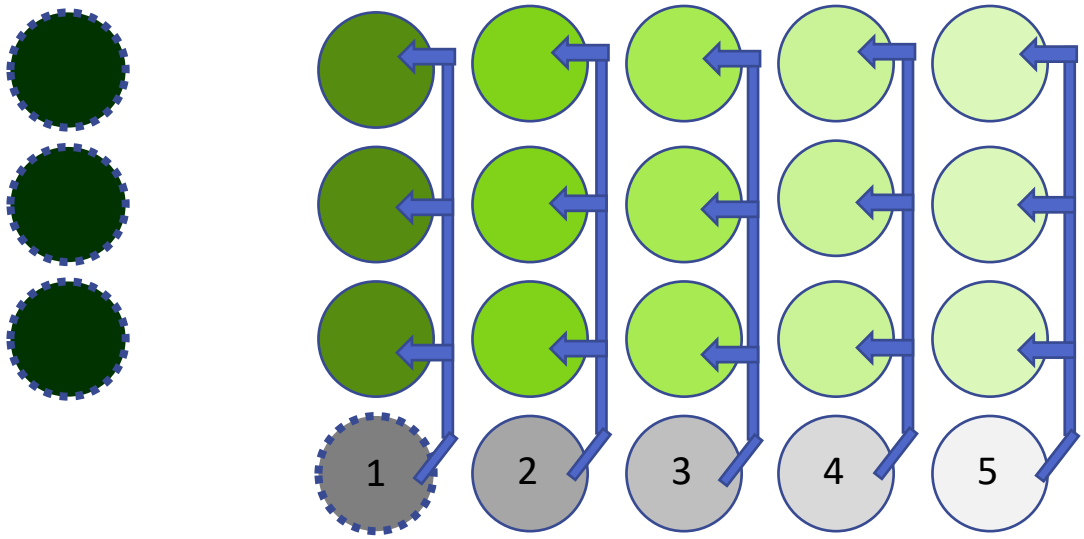

Figure 4. Diagram of Most Probable Number (MPN) Analysis. Green circles represent tubes filled with 10 mL of APW, an aqueous growth media. Gray circles represent tubes filled with 9 mL of PBS, a media used to resuspend samples but does not promote growth. First, 1 mL aliquots of sample are added to tubes with dashed borders. After vortexing, 1 mL of liquid from tube 1 is transferred to tube 2. After vortexing, 1 mL of liquid from tube 2 is transferred to tube 3; this process is carried on for tube 4 and tube 5. This step creates the serial dilution of the sample. After preparing the serial dilution, 1 mL aliquots of tube 5 are transferred to each of the three APW tubes in the same column. This process is repeated for tube 4 -1, indicated by the blue arrows.

2.5 Real-time PCR

Vibrio parahaemolyticus was detected using the target gene *tlh*, and *Vibrio vulnificus* was detected using the target gene *vvh,* both assays included an internal amplification control (Kinsey et al. 2015). Real-time PCR assays were conducted on the ABI 7500 Fast (Life Technologies, Foster City, CA). Each reaction contained 23 µL of mastermix and 2 µL of DNA template. Mastermix contained PCR Buffer, $MgCl_2$, dNTPs, forward and reverse primers, probes, Taq polymerase, and internal control DNA (Table

3). The *Vibrio vulnificus* cycling protocol started with 1-minute at 95°C followed by 45 cycles of 15 s at 95°C, 15 s at 57°C, and 25 s at 72°C. The *Vibrio parahaemolyticus* cycling protocol started with 1-minute at 95°C followed by 45 cycles of 5 s at 95°C and 45 s at 57°C. Data analysis was using default analysis parameters, except the manual threshold was changed to 0.02 and the background end cycle was set to 10 for all targets.

Table 3. PCR mastermix reagents and volumes for *Vibrio parahaemolyticus* and *Vibrio vulnificus* assays. JOE is 2′,7′-dimethoxy-4′,5′-dichloro-6-carboxyfluorescein. Cy5 is a fluorescent cyanine dye. BHQ1 and BHQ2 are Black Hole Quenchers 1 and 2, respectively. *V. vulnificus* primer sequences were originally reported by Campbell and Wright 2003, and *V. parahaemolyticus* primer sequences were reported by Nordstrom et al. 2007.

Component	Details/ Sequences (5' to 3')	Source	Final Concentration	Used in Vp mastermix	Used in Vv mastermix
PCR Water		Invitrogen	-	12.765 µL/rxn	12.220 µL/rxn
PCR Buffer		Invitrogen	1 X	X	X
$MgCl_2$	50 mM stock	Invitrogen	5.0 mM	X	X
dNTPs	Mixed equal concentrations of each	Roche, Indianapolis, IN	0.3 mM	X	X
tlh 884 F forward primer	ACTCAACACAAGAAGAGATCGACCA	Integrated DNA Technologies (IDT), Coralville IA	0.2 µM	X	
tlh 1091 R reverse primer	GATGAGCGGTTGATGTCCAA	IDT	0.2 µM	X	
vvh forward primer	TGTTTATGGTGAGAACGGTGACA	IDT	0.3 µM		X
vvh reverse primer	TTCTTTATCTAGGCCCCAAACTTG	IDT	0.3 µM		X
IAC 46 F forward primer	GACATCGATATGGGTGCCG	IDT	0.08 µM	X	X
IAC 186 R reverse primer	CGAGACGATGCAGCCATTC	IDT	0.08 µM	X	X
tlh probe	CGCTCGCGTTCACGAAACCGT Modifications: 5' JOE – 3' BHQ2	IDT	0.15 µM	X	
vvh probe	CCGTTAACCGAACCACCCGCAA Modifications: 5' Cy5 – 3' BHQ2	IDT	0.2 µM		X
IAC Cy5 probe	TCTCATGCGTCTCCCTGGTGAATGTG Modifications: 5' Cy5 - 3' BHQ2	IDT	0.15 µM	X	
IAC JOE probe	CGCTCGCGTTCACGAAACCGT Modifications: 5' JOE – 3'BHQ1	IDT	0.15 µM		X
Taq Polymerase	U Platinum *Taq* DNA Polymerase	Invitrogen	Vp- 1.5 unit/µL Vv- 1.2 unit/µL	0.30 µL/rxn	0.22 µL/rxn
Passive Reference Dye	ROX	ThermoFisher, Waltham, MA	-	X	X
Internal Amplification Control DNA (IAC)		Patent referenced in Nordstrom et al. 2007	-	X	X

2.6 Phytoplankton Identification

Preserved 1L samples were processed by the Alabama Department of Public Health (ADPH) Phytoplankton Unit.. The ADPH lab primarily monitors for larger dinoflagellates and harmful-algal-bloom forming species in coastal waters – notably *Dinophysis* spp., *Pseudo-nitzschia* spp., *Karenia brevis*, *Gonyaulax* spp., and cyanobacteria. Not all phytoplankton groups were identified and counted. Target genera cells in a representative sample aliquot were visually identified and enumerated using light microscopy. A concentration factor of 103 was used to scale subsample cell density to estimated cell density/L (Liefer et al. 2013; MacIntyre et al. 2011).

2.7 Statistical Analysis

MPN values were determined for each size fraction of each sample using a standard MPN table (Blodgett 2020); these values were then averaged for each site. Samples non-detectable by PCR for all MPN tubes were considered below the Limit of Detection (LOD; <30 MPN/L). For averaging, these samples were assigned a value of 15 MPN/L. Combined, or summed, *Vibrio* spp. abundances were determined by summing the three average vibrio abundances at each size fraction.

Spearman's non-parametric rank-based correlations were conducted to determine if any monotonic relationships existed between meteorological parameters (wind direction, wind speed, wind vectors), hydrographic variables (temperature, salinity, turbidity, nitrates/nitrites (NO_x), dissolved reactive phosphorus (DRP), ammonia, chlorophyll a, alkalinity), biological parameters (phytoplankton species abundances), and

Vibrio spp. abundances. Hydrographic parameters were tested against *Vibrio* spp. abundance associated with particles >35 μm, *Vibrio* spp. abundance associated with particles between 35 and 5 μm, *Vibrio* spp. abundance associated with particles < 5 μm, and *Vibrio* spp. abundance across size fractions (summed abundance). Meteorological and biological parameters were tested against *Vibrio* spp. abundance across size fractions. Spearman's correlations were used to help refine variables to include in subsequent linear mixed effects models and PERMANOVA analysis.

Linear mixed effects (LME) models were calculated to determine significant environmental predictors of *Vibrio* spp. abundances after accounting for site-based variation. LME models were created in R using the *nlme* package for summed vibrio abundances. Site was coded as a random effect, with environmental correlates (temperature, salinity, N-S wind vector, E-W wind vector, euphotic zone depth, turbidity, NO_x, DRP, chlorophyll a, total suspended solids (TSS), and ammonia) included in a global model as fixed effects. Correlations between fixed-effect variables were evaluated using the *car* package. All iterations of fixed effects within the global model were evaluated using the 'dredge' function within the *MuMIn* package to determine the best fit model. The best fit model output was then assessed with an analysis of variance (ANOVA) to determine R^2 values attributed to fixed effects and random effects in the model. This process was completed for *Vibrio vulnificus* and *Vibrio parahaemolyticus* summed abundances.

PERMANOVA and non-metric NMDS approaches were used to determine environmental variables that structure planktonic communities (i.e., *Vibrio* spp. and harmful algal groups) in the sampling region. These analyses were calculated by using

the *vegan* package in R. Environmental correlates were reduced to 2 dimensions in the NMDS analysis and were plotted using the *ggplot2* package. The PERMANOVA was completed using the 'adonis' function and was set to run with 999 permutations. Vectors were calculated using the 'envfit' function and were overlain onto the NMDS plot.

CHAPTER 3 RESULTS

3.1 Meteorology

As expected, meteorological parameters such as wind direction, wind speed, precipitation, and freshwater discharge from the Mobile-Tensaw delta varied throughout the study period. The mean wind direction during the year was south-southeast (Figure 5a). Wind speed showed some seasonal trends, with lower average wind speeds occurring during the summer months (May - Sept) (Figure 5b). In contrast to the dominant annual wind direction, for the sampling days from April to October 2019, northeast winds were the most frequent (Figure 5c). Wind speeds recorded during the sampling period ranged from 1.22 m/s to 15.41 m/s.

The Dauphin Island ARCOS meteorological station recorded 137.7 centimeters of rain in 2019, with the most intense rainfall events occurring in the months of April-July (Figure 6a). The pulses of rainfall align with increases in the freshwater discharge from the Mobile and Tensaw Rivers (Figure 6b), major tributaries to the Mobile-Tensaw Delta in northern Mobile Bay. Freshwater discharge remained above 900 m^3/s for each river from January - May, which were the highest rates of the year (Figure 6b and data not shown).

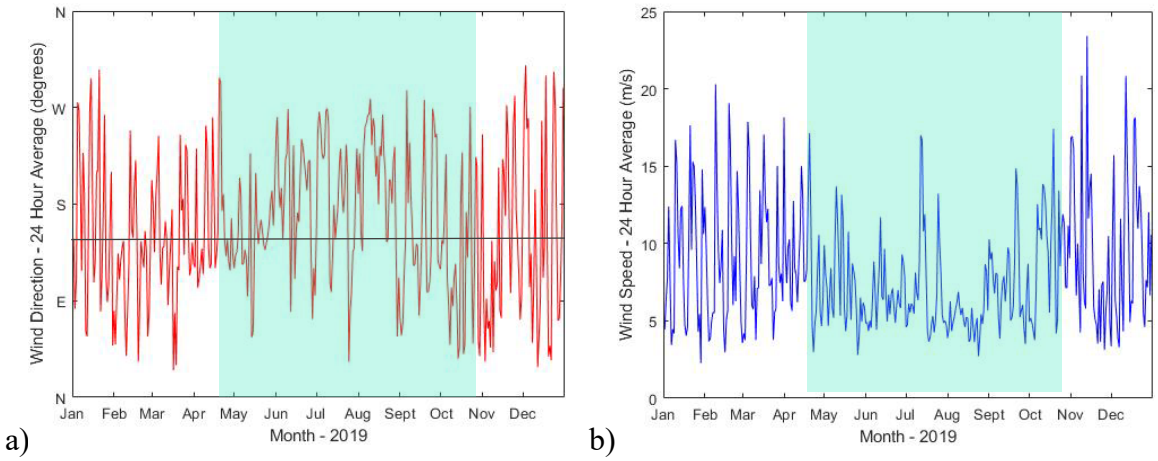

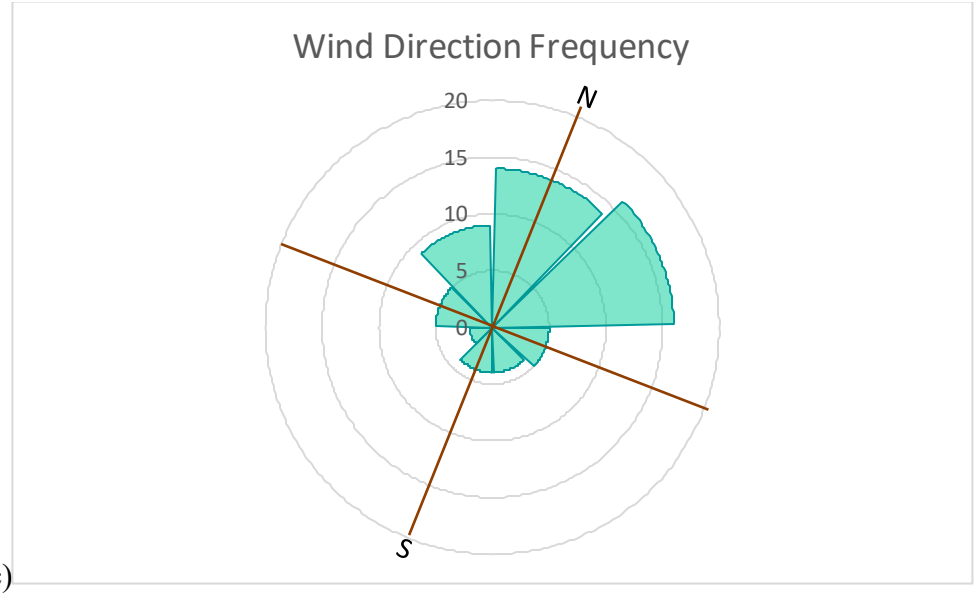

Figure 5. Wind data trends in the Eastern Mississippi Sound System. **a)** Daily average wind direction for 2019 – recorded in meteorological notation by the Dauphin Island ARCOS meteorological station. Sampling period is indicated by the shaded blue box. The mean wind direction (SSE) is indicated by the black line. **b)** Daily average wind speed (m/s) for 2019 – recorded by the Dauphin Island ARCOS meteorological station. Sampling period is indicated by the shaded blue box. **c)** Rose diagram of wind direction frequency on sampling days (April -October 2019).

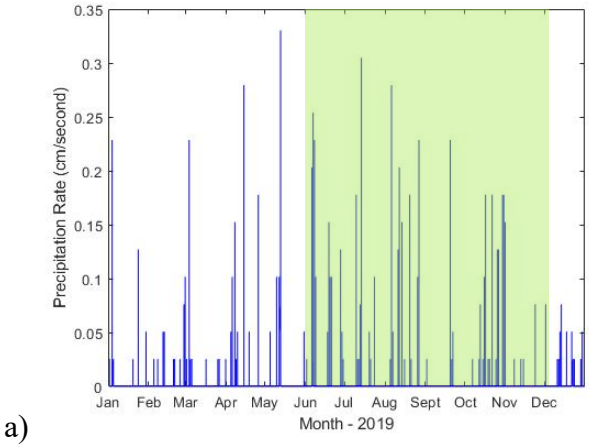

a)

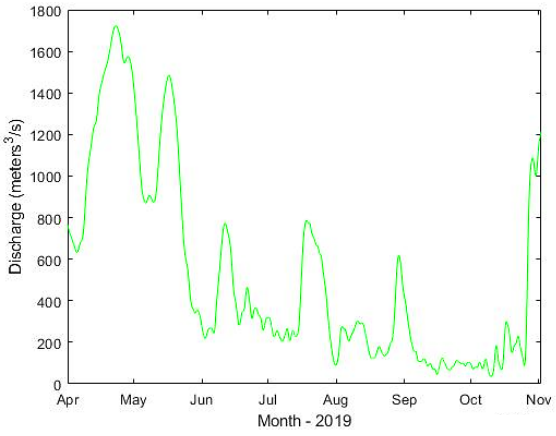

b)

Figure 6. Precipitation and river discharge trends in 2019. **a)** Precipitation rate recorded by the Dauphin Island ARCOS meteorological station. **b)** freshwater discharge rate for the Mobile River during the sampling period, recorded by USGS river gauge station #02470629 in Bucks, AL. The green rectangle indicates the sampling period. Magnitude and intensity of freshwater discharge was mirrored by the Tensaw River as recorded by the USGS river gauge station #02471019 in Mt. Vernon, AL (data not shown). Discharge volumes were filtered to remove the effects of tidal forcing.

3.2 Hydrography

The near-continuous ARCOS hydrography station on Dauphin Island recorded a temperature range between 15.8 and 33.3 °C, salinity between 1.9 and 32.9 ppt, and turbidity (24-hour average) between 5.1 and 121 NTU during the sampling period (Figure 7). Among the 10 sites and specific days sampled, the ranges were lower: temperature varied between 20.0 and 31.0°C, salinity between 4.8 and 32.7 ppt, and turbidity between 0.4 and 39.4 NTU (Figure 8 and 9). Temperature fluctuated seasonally, with the lowest recordings at the beginning and end of the sampling window (April-May, and October) (Figure 7a). Salinity displayed a seasonal trend, with lowest values in the early sampling months (Figure 7b); this is expected, due to intense freshwater inputs earlier in the hydrographic year (Figure 6). Turbidity did not display any overt seasonal trends (Figure 7c). Salinity and turbidity measurements taken in situ at sampling stations were negatively correlated ($\rho_s = -0.595$, $p < 0.001$). This negative correlation is mirrored in the continuous water quality ARCOS station on Dauphin Island; high turbidity events were typically preceded by notable drops in the salinity (within a 3-day period). Salinity trends seen at sampling sites in the EMSS (Figure 8) followed a similar pattern (low salinities in April-June, then increasing to moderate salinities). Temperature at sites in the EMSS also followed a standard trend, with lowest temperatures at the beginning (April) and end of the sampling season (October) (Figure 9 a-c). Turbidity did not follow any seasonal patterns (Figure 9 d-f).

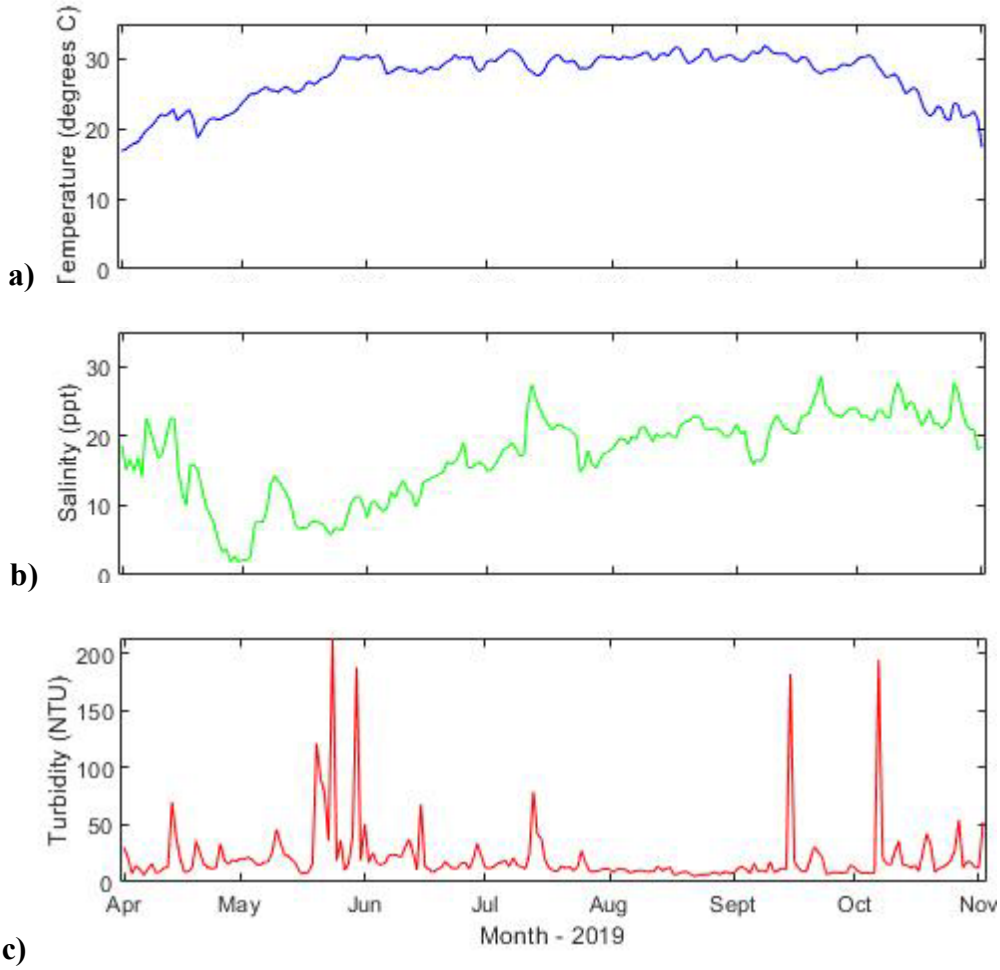

Figure 7. Hydrographic data, **a)** temperature, **b)** salinity, and **c)** turbidity, collected from the Dauphin Island ARCOS hydrographic station concurrently with the sampling period in the EMSS.

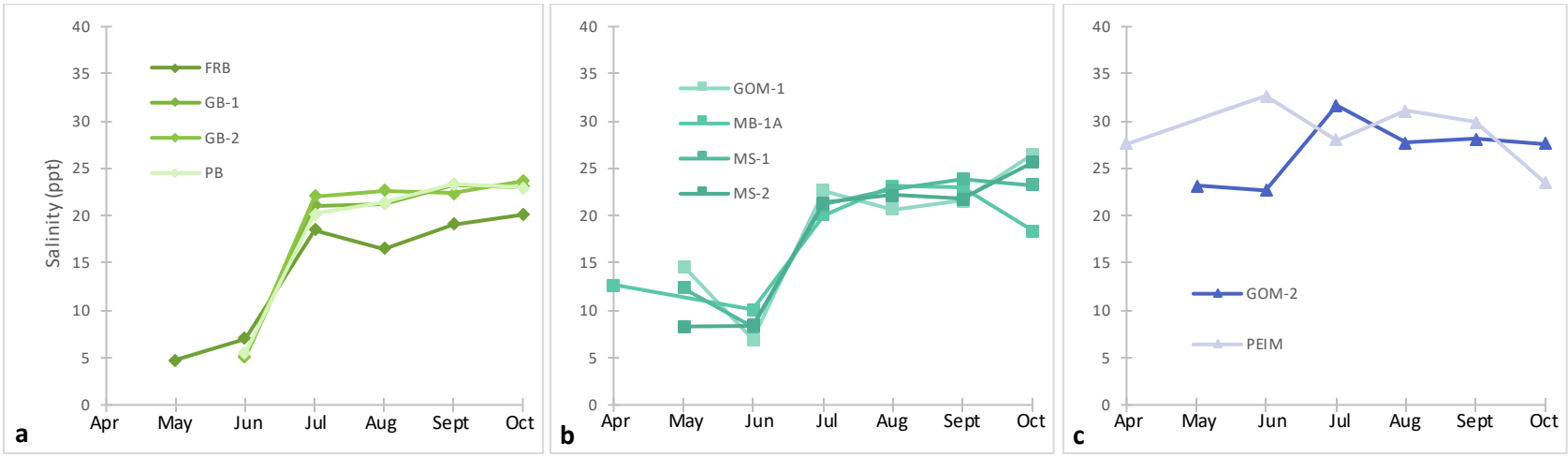

Figure 8**.** Salinity (**a-c**) trends at sampling sites in the Eastern Mississippi Sound System. Points indicate the single sampling point for each month. Green diamond markers indicate the northernmost coastal bay sites. Teal square markers indicate central sound sites. Blue triangle markers indicate southernmost barrier island sites.

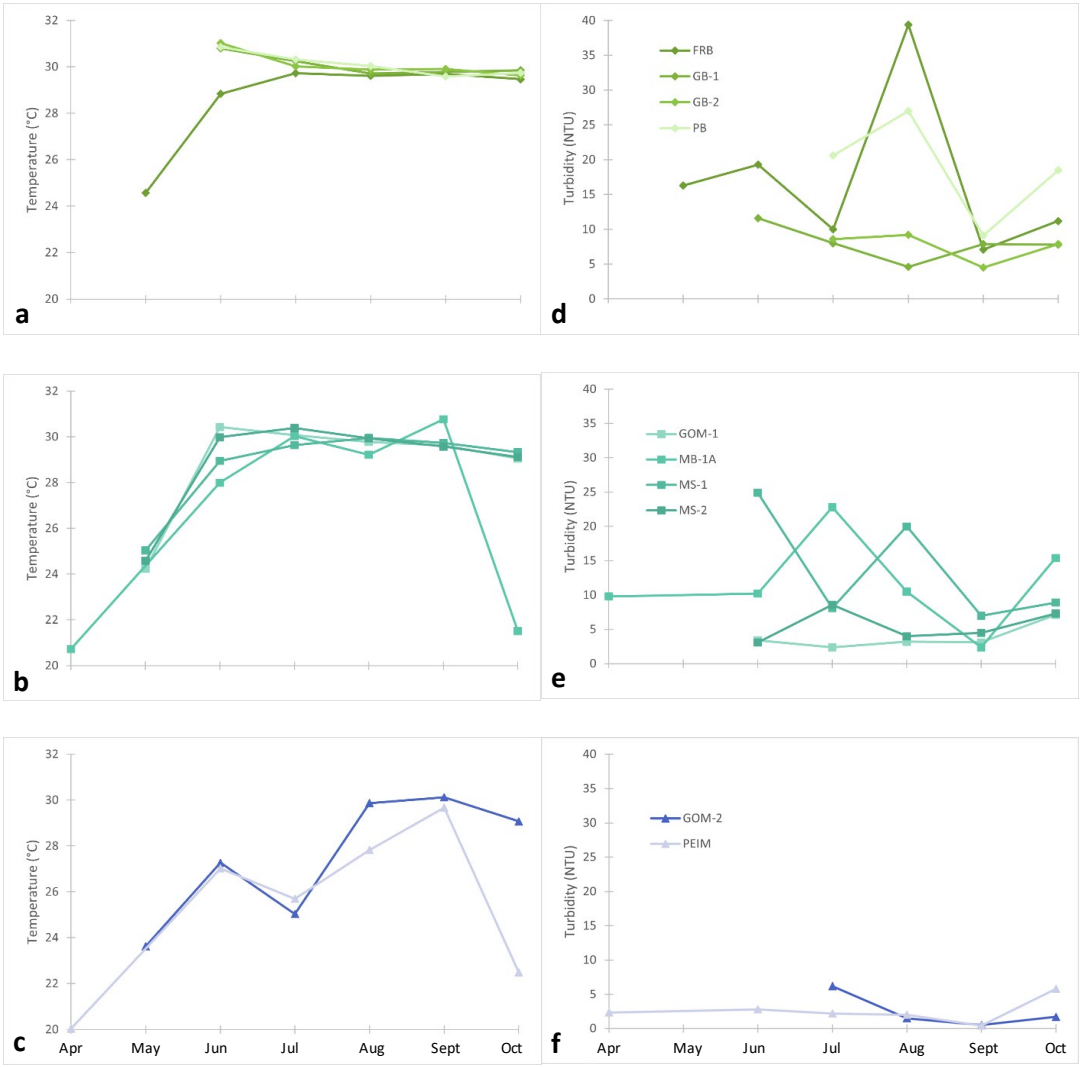

Figure 9. Temperature (**a-c**) and turbidity (**d-f**) trends at sampling sites in the Eastern Mississippi Sound System. Points indicate the single sampling point for each month. Green diamond markers indicate the northernmost coastal bay sites. Teal square markers indicate central sound sites. Blue triangle markers indicate southernmost barrier island sites

3.2.1 Nutrients

Many samples yielded nutrient concentrations at or below the limit of detection (72% of NO_x samples, 70% of DRP samples). Sites with greater marine influence (GOM-2, GOM-1, and PEIM) tended to have higher NO_x concentrations (> 0.04 mg/L) than near-shore sites throughout the sampling period. Dissolved reactive phosphorus (DRP) did not yield any clear trends across sites (Figure 10). From May to October, ammonia levels consistently exceeded the maximum concentration of quantitation by ADEM methods (0.09 mg/L) across all sites. Salinity was not significantly correlated with ammonia (NH_3), nitrate/nitrite (NO_x), or DRP (NH_3: ρ_s=0.22, p= 0.09; NO_x: ρ_s=0.17, p= 0.20; DRP: ρ_s=0.06, p= 0.67).

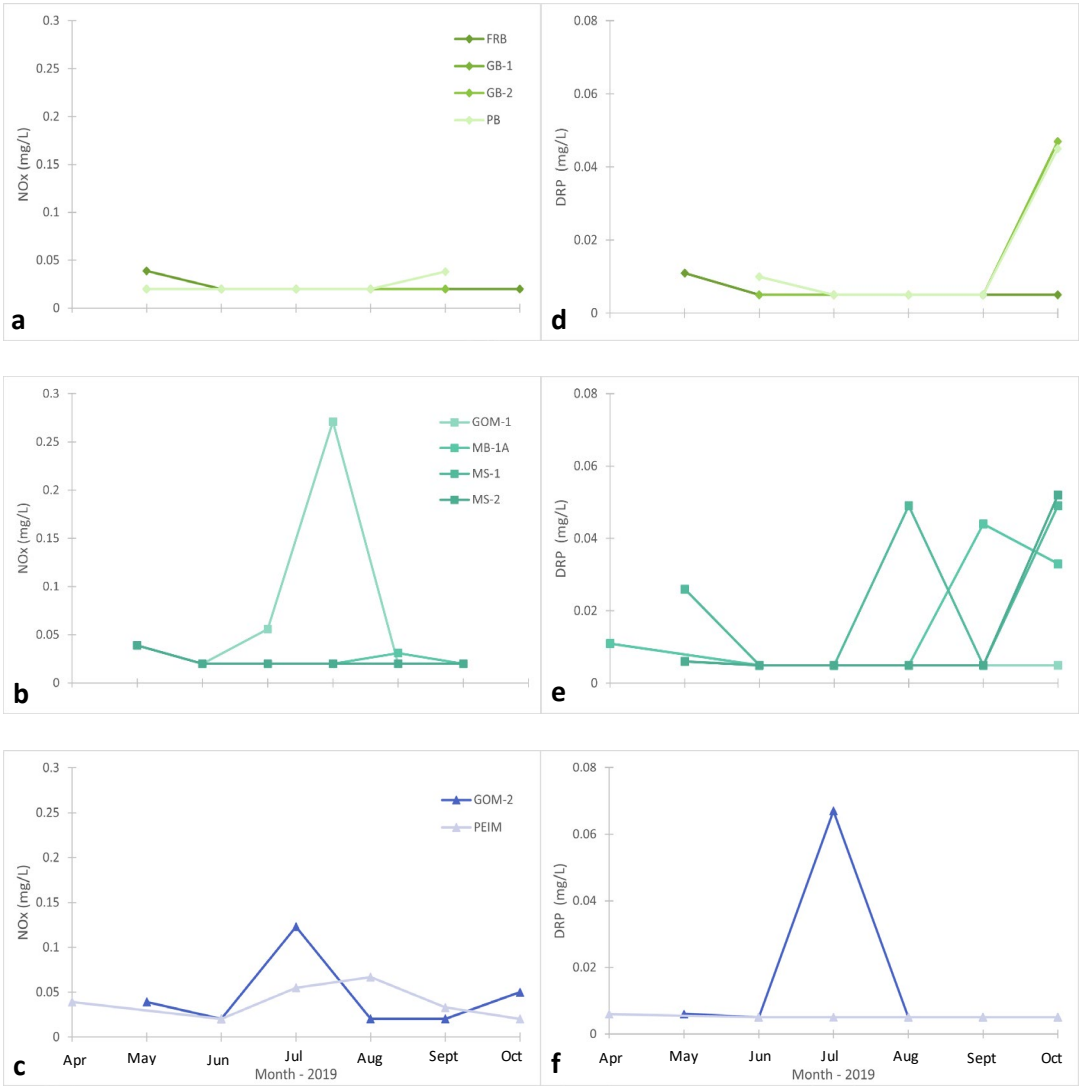

Figure 10. Nutrient trends at sampling sites in the Eastern Mississippi Sound System. Nitrate and nitrite concentrations (NOx) are shown in the left column (**a-c**); dissolved reactive phosphorus concentrations are shown in the right (**d-f**). Plots are grouped by region: green indicates coastal bay sites (FRB, GB-1, GB-2, and PB), teal indicates sound sites (MS-1, MS-2, GOM-1, and MB-1A), and blue indicates barrier island sites (GOM-2 and PEIM)

3.3 Biology

3.3.1 Harmful Algal Diversity

Thirty-three species of potentially harmful algae were identified and enumerated by the Alabama Department of Public Health from June – October of the sampling period. The species belonged to 18 genera, with dinoflagellates having the greatest diversity. Some species were only recorded once (i.e., *Diplopsalis lenticula, Katodinium glaucum, etc.*), whereas others were recorded throughout the sampling period (*Protoperidineum* spp., *Ceratium hircus, Prorocentrum scutellum*, etc.). Many species were only found within specific salinity conditions (Figure 11). Cell densities greater than 15,000 cells/L of *Akashiwo sanguinea*, *Prorocentrum micans*, and *Pseudo-nitzschia spp*. were reported in June at site GB-2, August at site MS-2, and September at site PEIM, respectively.

3.3.2 Chlorophyll a and Microplankton Abundances

Chlorophyll a concentration ranged widely throughout the sampling season and did not yield any clear trends among sites (Figure 12 a-c). Chlorophyll a concentrations ranged from 1 µg/L (limit of detection) to 7.4 µg/L during the sampling period. Harmful algal abundances ranged from 100 to 48,000 cells/L. Chlorophyll a measurements also did not generally trend with these[a] cell abundances (Figure 12d). Such a lack of correlation ($\rho_s = 0.20$, $p = 0.20$) may imply a significant detrital chlorophyll signature at sites in the EMSS or that the chlorophyll a signal was primarily driven by phytoplankton which are not recognized as harmful algal species.

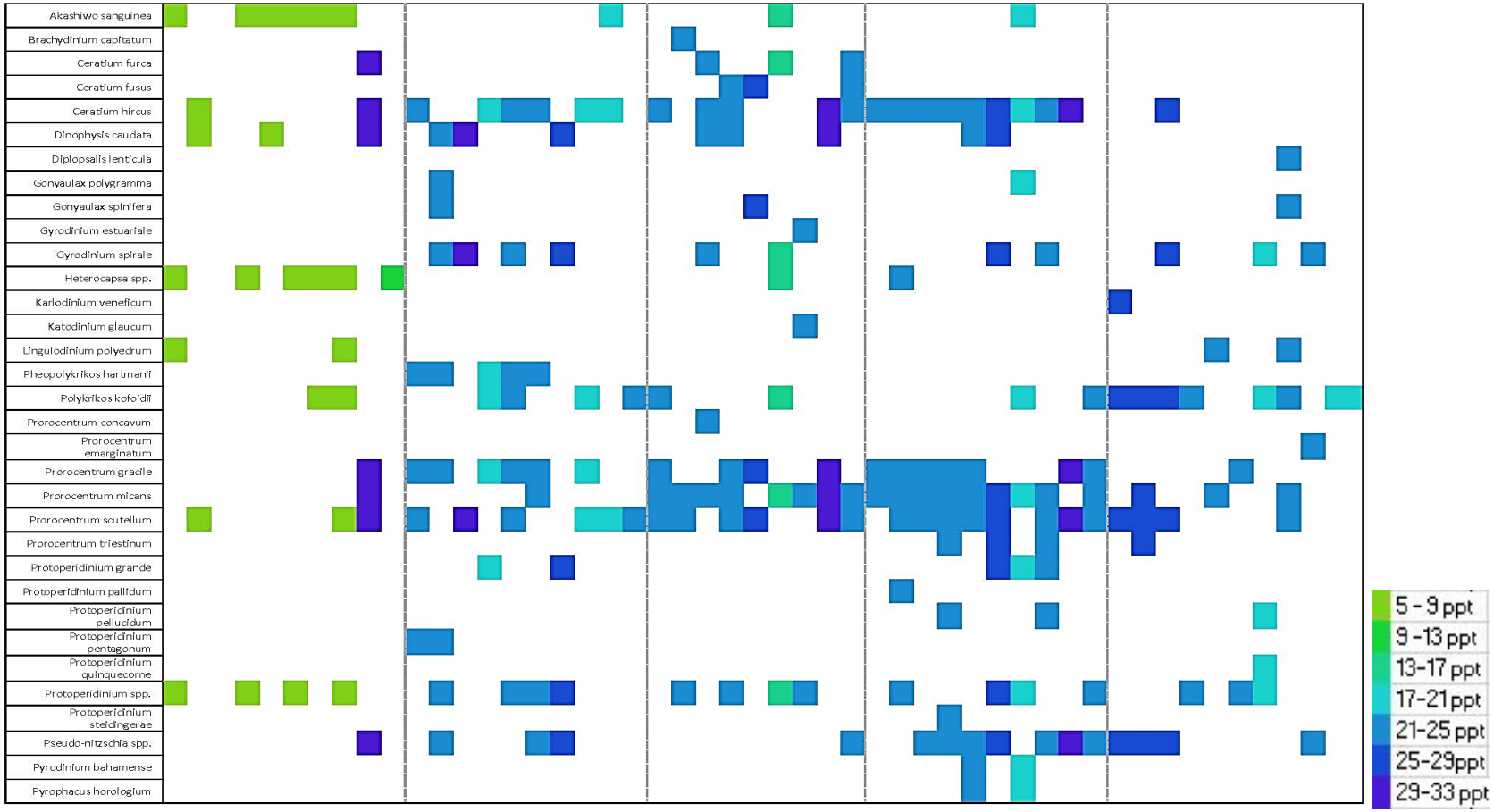

Figure 11. Heat map of phytoplankton occurrence and associated salinity. Shaded squares indicate samples where a certain species was recorded; the color of the square signifies the salinity at the site when the species was found.

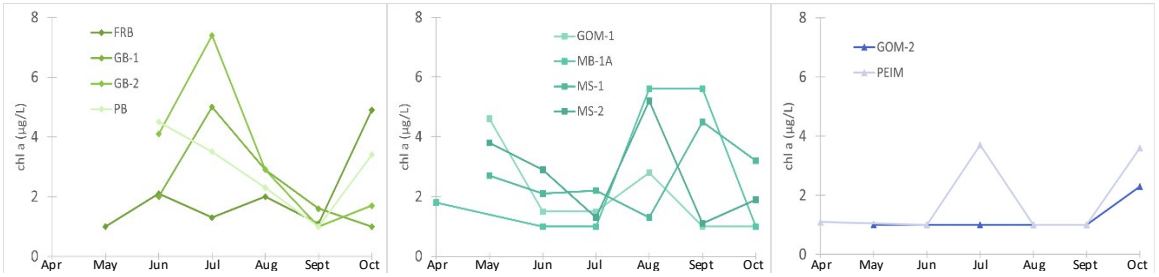

d

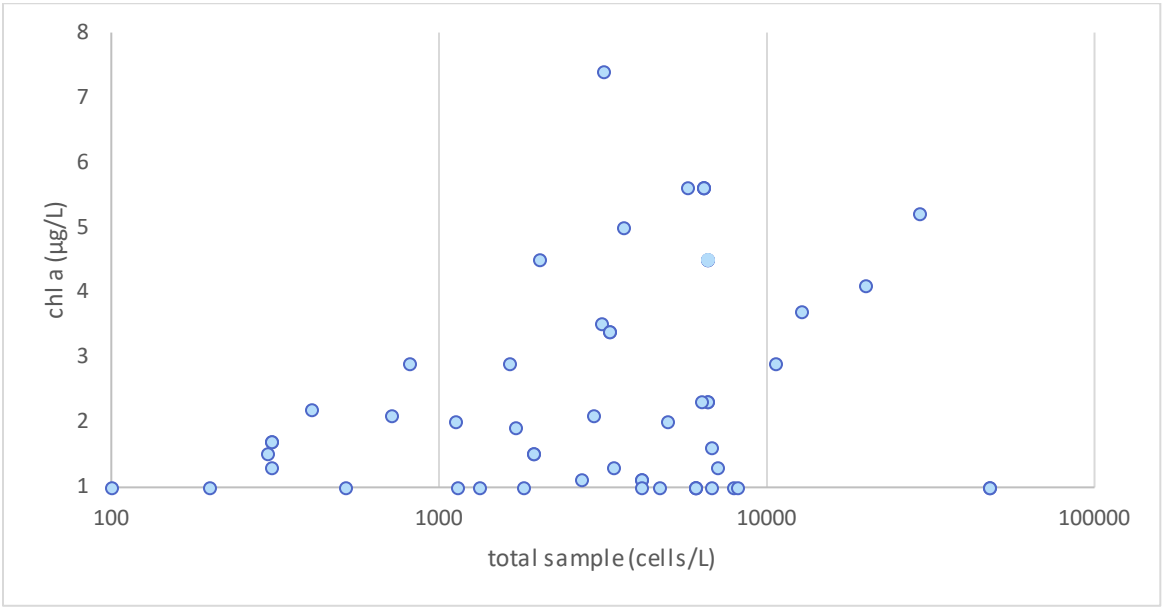

Figure 12**. a-c)** Chlorophyll a measured among sites in the EMSS. Plots in green indicate coastal bay sites, plots in teal indicate sound sites, and plots in blue indicate barrier island sites. **d)** Chlorophyll a concentrations plotted against harmful algal abundances (log transformed). Limit of detection for chlorophyll a was 1 µg/L.

3.3.3 Vibrio

Vibrio spp. abundances were determined for each size fraction of water >35 μm, 35-5 μm, and <5 μm to infer associations with particles of various sizes. The abundances determined for each size fraction at each sampling time and location were summed to provide a combined abundance. *Vibrio* spp. abundances fluctuated throughout the sampling period and across sites, with the highest mean combined abundances at FRB, MB-1A, PB, GB-1, and MS-1 (Figure 13). *Vibrio parahaemolyticus* abundances ranged from < 90 MPN/L (limit of detection) to 9441 MPN/L, with a median value of 202 MPN/L. *Vibrio vulnificus* abundances varied between < 90 MPN/L (limit of detection) and 123,615 MPN/L, with a median value of 798 MPN/L.

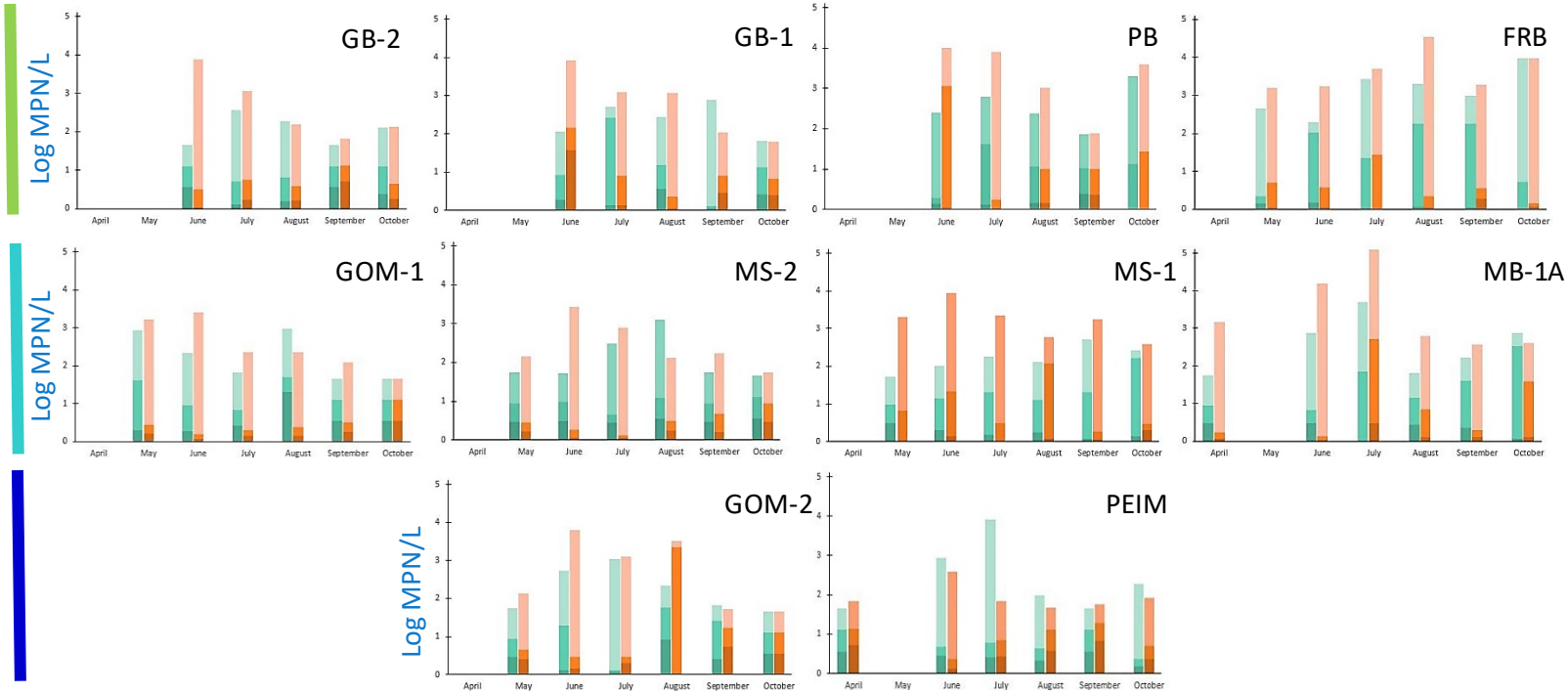

Figure 13. *Vibrio* spp. abundances at each site across the sampling period (April – October 2019). Plots are arranged by site region (see colored bars) and go from west to east. *Vibrio parahaemolyticus* abundances are plotted in teal and *Vibrio vulnificus* abundances are plotted in orange. The darkest shaded areas on the stacked bar graph indicate vibrios associated with the largest size fraction (35 µm or greater). The medium shaded areas indicate vibrio abundance associated with the middle size fraction (35 – 5 µm). The lightest shaded areas indicate vibrio abundance associated with the smallest size fraction (less than 5 µm). Please note the y- axis reflects log (base 10) transformed MPN/L values.

On average, 30 – 50% of total *Vibrio* spp. in any sample was associated with particles equal to or larger than 5 µm (Table 4). These particles could be living planktonic organisms (phytoplankton and zooplankton), organic detritus, or sediment grains. The distribution of *Vibrio vulnificus* associated with particles appeared to be related to salinity (Figure 14a). *Vibrio vulnificus* was primarily associated with smaller particles in lower salinities (median, 11ppt) and larger particles in higher salinities (median, 22 ppt), indicating significantly different particle association patterns in relation to salinity (Kruskal-Wallis test: $H = 4.13$, $p = 0.04$). This relationship did not exist for *Vibrio parahaemolyticus*. Turbidity did not significantly affect particle size interactions for either species (Figure 14b).

Table 4. Average proportion (±standard error) of bacteria associated with particles at each size fraction. Size fractions consist of particles ≥ 35 µm, particles between 35 and 5 µm, and particles <5 µm.

Size fraction	Vp	Vv
≥ 35 µm	0.16 ± 0.02	0.12 ± 0.02
35 - 5 µm	0.35 ± 0.03	0.21 ± 0.02
<5 µm	0.49 ± 0.03	0.67 ± 0.03

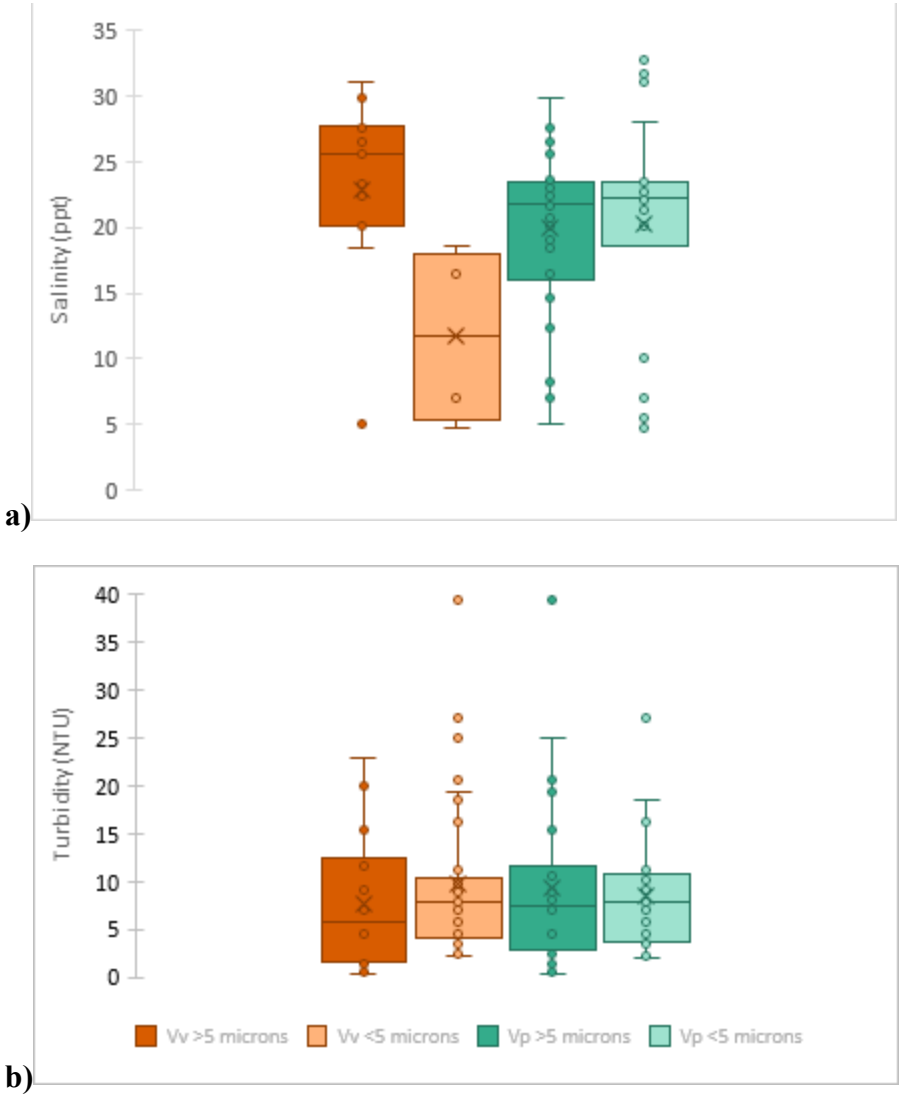

Figure 14.**a)** *Vibrio* spp. associations with size fractions of particles with respect to salinity. The median salinity when the majority of *Vibrio vulnificus* is associated with particles >5µm is 22 ppt and the median salinity when the majority of *Vibrio vulnificus* is associated with particles < 5µm is 11 ppt. *Vibrio parahaemolyticus* - particle size association does not appear to be affected by salinity. **b)** *Vibrio* spp. associations with size fractions of particles with respect to turbidity. Particle size association does not appear to be affected by turbidity for either vibrio species.

3.4 Statistical Evaluation

3.4.1. Correlation Analyses

3.4.1.1 Meteorology. Summed *Vibrio vulnificus* and *Vibrio parahaemolyticus* counts generally did not trend with raw wind direction or wind speed, except for summed Vp and raw wind direction (ρ_s =0.28, p = 0.03). No other significant correlations were observed. However, when compared with wind scalars (the N-S and E-W components of the wind), both *Vibrio vulnificus* abundances and *Vibrio parahaemolyticus* abundances displayed a negative correlation with the E-W wind scalar (Table 5). Winds from the west were correlated to an increase in *Vibrio* spp. abundance, whereas winds from the east were correlated to a decrease in *Vibrio* spp. abundance. These patterns became weaker over an 8-hour time frame but were still significant over a 24-hour timeframe.

Table 5. Spearman's ρ (p values in parentheses, significant values **bold**) between summed *Vibrio vulnificus* (Vv) and *Vibrio parahaemolyticus* (Vp) abundances and wind scalars. In situ refers to the wind scalars during the time of sampling. The 8-hour average refers to winds occurring during an 8-hour period prior to sampling. The 24-hour average refers to winds occurring during a 24-hour period prior to sampling. Note: 8-hour E-W correlation with Vv is not significant (i.e., rounded down to 0.05).

	In situ	In situ	8-hour average	8-hour average	24-hour average	24-hour average
Species	N-S scalar	E-W scalar	N-S scalar	E-W scalar	N-S scalar	E-W scalar
Vv	-0.09 (0.50)	-0.30 **(0.03)**	0.02 (0.86)	-0.26 (0.05)	-0.09 (0.48)	-0.38 (**<0.01**)
Vp	0.06 (0.64)	-0.26 **(0.05)**	0.20 (0.14)	-0.22 (0.10)	0.05 (0.73)	-0.33 (**0.01**)

3.4.1.2 Hydrography and Nutrients. Spearman's ρ were calculated for each hydrographic variable and *Vibrio* spp. abundances (Table 6). There was a significant negative correlation between *Vibrio vulnificus* and salinity across all size fractions and combined abundances. *Vibrio parahaemolyticus* abundances did not have significant correlations with salinity. Although temperature has been shown to be a significant predictor of *Vibrio* spp. abundance in past studies (Randa et al. 2004, Turner et al. 2009), there was no significant correlation to temperature for either species in our sampling period as these months had optimal temperature conditions for *Vibrio* spp. growth. Both species were positively correlated with turbidity. Combined *V. vulnificus* abundances were negatively correlated with NO_x. Combined *V. parahaemolyticus* and Vp abundances in the <5 μm size fraction were positively correlated to alkalinity. All vibrio abundances except *Vibrio parahaemolyticus* in the 35 μm size fraction were negatively correlated to euphotic zone depth.

Table 6. Spearman's ρ (p values) for hydrographic variables, *Vibrio parahaemolyticus*, and *Vibrio vulnificus*. Significant correlations are bolded. NO_x includes nitrates and nitrites. DRP is dissolved reactive phosphorus and NH_3 is ammonia. P-values were rounded, hence some 0.05 reported were not significant.

	Vp				Vv			
	>35 μm	5-35 μm	<5 μm	Σ	>35 μm	5-35 μm	<5 μm	Σ
Salinity	-0.04	-0.19	-0.16	-0.16	-0.37	-0.58	-0.66	-0.65
	(0.76)	(0.15)	(0.25)	(0.25)	**(<0.01)**	**(<0.01)**	**(<0.01)**	**(<0.01)**
Temperature	0.00	0.13	0.03	0.05	0.15	0.21	0.21	0.23
	(0.99)	(0.33)	(0.81)	(0.70)	(0.27)	(0.12)	(0.11)	(0.09)
Turbidity	-0.13	0.42	0.29	0.36	0.37	0.69	0.59	0.59
	(0.21)	**(<0.01)**	**(<0.01)**	**(<0.01)**	**(<0.01)**	**(<0.01)**	**(<0.01)**	**(<0.01)**
NO_x	0.08	-0.26	-0.01	-0.09	-0.19	-0.32	-0.24	-0.28
	(0.55)	(0.05)	(0.92)	(0.51)	(0.16)	**(0.01)**	(0.07)	**(0.04)**
DRP	-0.13	-0.15	-0.12	-0.10	-0.13	-0.04	-0.12	-0.10
	(0.35)	(0.28)	(0.38)	(0.48)	(0.35)	(0.78)	(0.38)	(0.46)
NH_3	0.05	0.26	0.16	0.22	0.00	0.09	0.03	0.03
	(0.69)	(0.05)	(0.25)	(0.10)	(0.98)	(0.50)	(0.80)	(0.80)
Alkalinity	0.21	-0.20	0.34	0.35	-0.21	-0.20	-0.25	-0.23
	(0.11)	(0.14)	**(0.01)**	**(0.01)**	(0.12)	(0.14)	(0.06)	(0.09)
Euphotic Zone Depth	0.15	-0.45	-0.31	-0.35	-0.36	-0.64	-0.59	-0.58
	(0.28)	**(<0.01)**	**(0.02)**	**(<0.01)**	**(<0.01)**	**(<0.01)**	**(<0.01)**	**(<0.01)**

40

3.4.1.3 Biology. Spearman's ρ were calculated between *Vibrio* spp. abundances and observed harmful algal genera (Table 7). *Vibrio vulnificus* abundances were significantly correlated to the abundances of dinoflagellates *Akashiwo sanguinea* and *Heterocapsa* spp. *V. vulnificus* also had significant negative correlations with the abundances of dinoflagellates *Prorocentrum* spp. and diatom *Pseudo-nitzschia* spp. *Vibrio parahaemolyticus* abundances only had a significant negative correlation with *Pseudo-nitzschia* spp. These relationships mirror correlations with salinity and turbidity (Table 6, Table 8) and potentially indicate community structure associated with freshwater input and the factors it affects (Figure 15). Additionally, none of the harmful algal species' abundances were correlated with bulk chlorophyll a.

Table 7. Spearman's ρ (p values) between phytoplankton groups and combined *Vibrio* spp. abundances. Bolded correlations are significant.

	Σ Vp	**Σ Vv**
Akashiwo sanguinea	-0.02 (0.92)	0.51 **(<0.01)**
***Ceratium* spp.**	0.15 (0.31)	-0.09 (0.54)
***Dinophysis* spp.**	-0.00 (0.98)	-0.23 (0.10)
***Heterocapsa* spp.**	-0.08 (0.60)	0.42 **(<0.01)**
Polykrikos kofoidii	0.06 (0.71)	0.18 (0.20)
***Prorocentrum* spp.**	-0.24 (0.09)	-0.44 **(<0.01)**
***Protoperidineum* spp.**	0.07 (0.65)	0.15 (0.30)
***Pseudo-nitzschia* spp.**	-0.33 **(0.02)**	-0.54 **(<0.01)**

Table 8. Spearman's ρ (p values) between phytoplankton abundances, hydrographic variables, and nutrients. Bolded correlations are significant.

Hydrographic Variable	*Akashiwo sanguinea*	*Heterocapsa* spp.	*Prorocentrum* spp.	*Pseudo-nitzschia* spp.
Salinity	-0.63 **(<0.01)**	-0.53 **(<0.01)**	0.44 **(<0.01)**	0.51 **(<0.01)**
Temperature	0.16 (0.26)	0.05 (0.71)	0.23 (0.11)	-0.13 (0.38)
Turbidity	0.31 **(0.03)**	0.29 **(0.05)**	-0.22 (0.15)	-0.53 **(<0.01)**
NO_x	-0.22 (0.13)	-0.20 (0.16)	-0.09 (0.52)	0.27 (0.06)
DRP	-0.13 (0.35)	-0.09 (0.52)	-0.16 (0.25)	-0.14 (0.33)

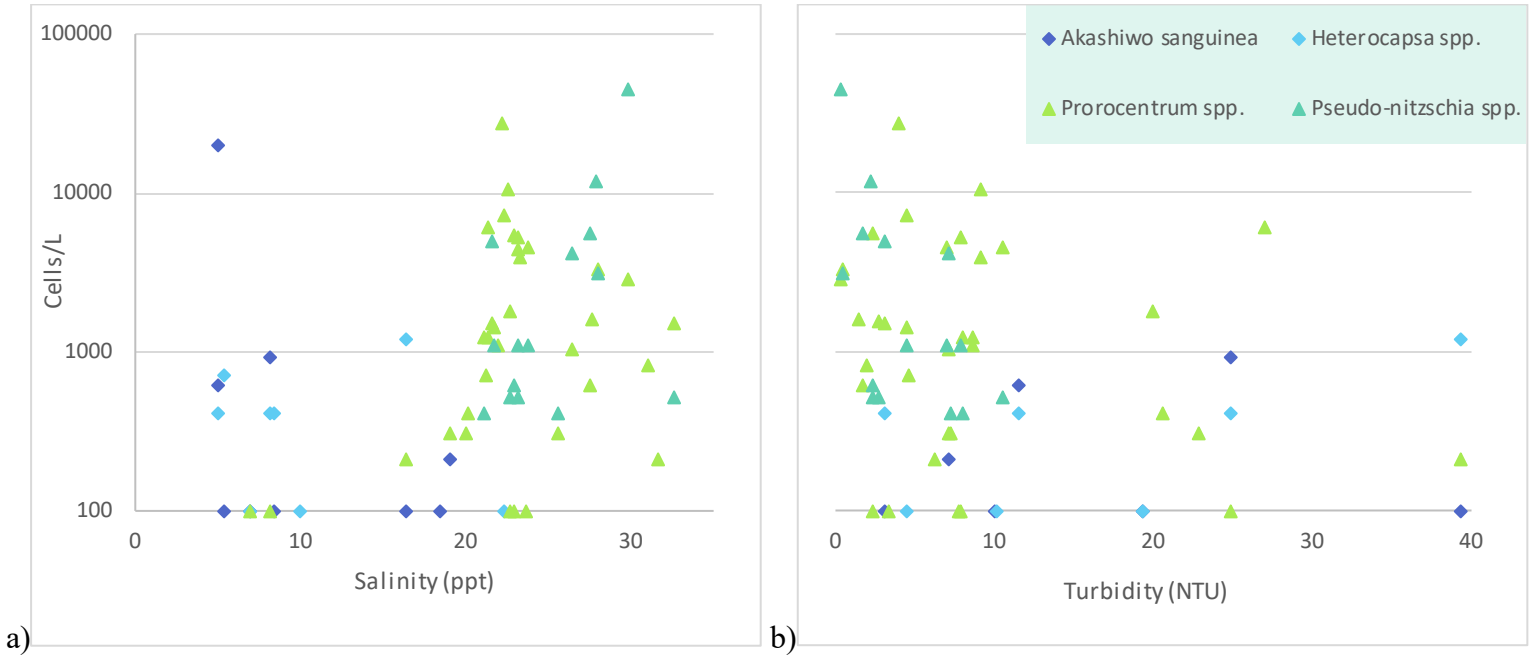

Figure 15. Visualization of low salinity/ high salinity and low turbidity/high turbidity correlated phytoplankton regimes. **a)** Plot of salinity and **b)** turbidity with harmful algae concentrations of *Akashiwo sanguinea*, *Heterocapsa* spp., *Prorocentrum* spp., and *Pseudo-nitzschia* spp. Diamonds indicate species associated with lower salinity and triangles indicate species associated with higher salinity.

Phytoplankton species that correlated with vibrios generally did not dominate community abundances. The genera that correlated with *Vibrio* spp., on average comprised 28% (*Akashiwo sanguinea*) to 45% (*Prorocentrum* spp.) of the phytoplankton community in their respective samples. These genera made up a majority of the phytoplankton community in less than 40% of all samples (*Heterocapsa* spp. – 13%; *A. sanguinea* – 22%; *Pseudo-nitzschia* spp. – 33%; *Prorocentrum* spp. – 38%).

3.4.2 Linear Mixed Effects (LME) Models

Linear mixed effects models were created for summed *Vibrio* spp. abundances. Accounting for the variance attributed to each of the environmental factors retained in the Vp best fit model (Table 9), salinity, N-S wind vector, DRP, and ammonia were the only significant predictors of *Vibrio parahaemolyticus* abundance. Almost all variation in *V. vulnificus* abundances can be attributed to site, whereas about 41% of variation in *V. parahaemolyticus* can be attributed to site. After accounting for the variance attributed to each of the environmental factors retained in the Vv best fit model, the N-S wind vector was the only significant predictor of *V. vulnificus* abundance. Similarly, fixed effect factors of salinity, N-S wind vector, DRP and NH3 all were significant predictors of *V. parahaemolyticus* abundance.

Table 9. Representation of fixed effects and significant parameters in best-fit linear mixed effects models for *Vibrio* spp. Shaded cells represent parameters that were retained in the best-fit model for each species. Asterisks indicate significant predictors, with triple asterisks indicating (p~0), double (p ~0.001), and single (p~0.01). R^2 values for fixed effects (R^2_{fe}) and for random effects (R^2_{re}) are reported in the last two columns. Fixed effects include model parameters and random effect is site.

Model	Temp	Sal	N-S wind vector	E-W wind vector	Euphotic zone	Turbidity	NOx	DRP	Chl a	Alkalinity	TSS	NH3	R^2_{fe}	R^2_{re}
Vp		*	**					***				***	0.16	0.41
Vv			**										~ 0	~ 1

3.4.3 NMDS and PERMANOVA

To determine the relationship between environmental variables and the structure of planktonic assemblages. After plotting the NMDS coordinates for each community sampled, no defined clusters were seen (Figure 16a). When species were plotted on top of the NMDS coordinates, species with higher salinity tolerances were grouped on the right half of the plot, whereas species with lower preferred salinities were grouped on the left side of the plot. These preliminary trends were confirmed by overlaying structuring variables on top of the NMDS plot as vectors. Significant structuring variables for these communities across site differences included temperature ($p<0.01$), salinity ($p<0.01$), euphotic depth ($p<0.01$), turbidity ($p<0.02$), and alkalinity ($p<0.02$). Vectors can be used as a sort of pseudo-axis; the value of the variable plotted on the vector increases moving from the center of the NMDS plot outwards. Using this logic, higher temperatures pull communities toward the top right quadrant of the NMDS ordination, higher salinities pull communities toward the bottom right quadrant, and higher turbidity pulls communities towards the top left quadrant. Length of the vector indicates the strength of the relationship; therefore, significant factors are the longest vectors (Figure 16b).

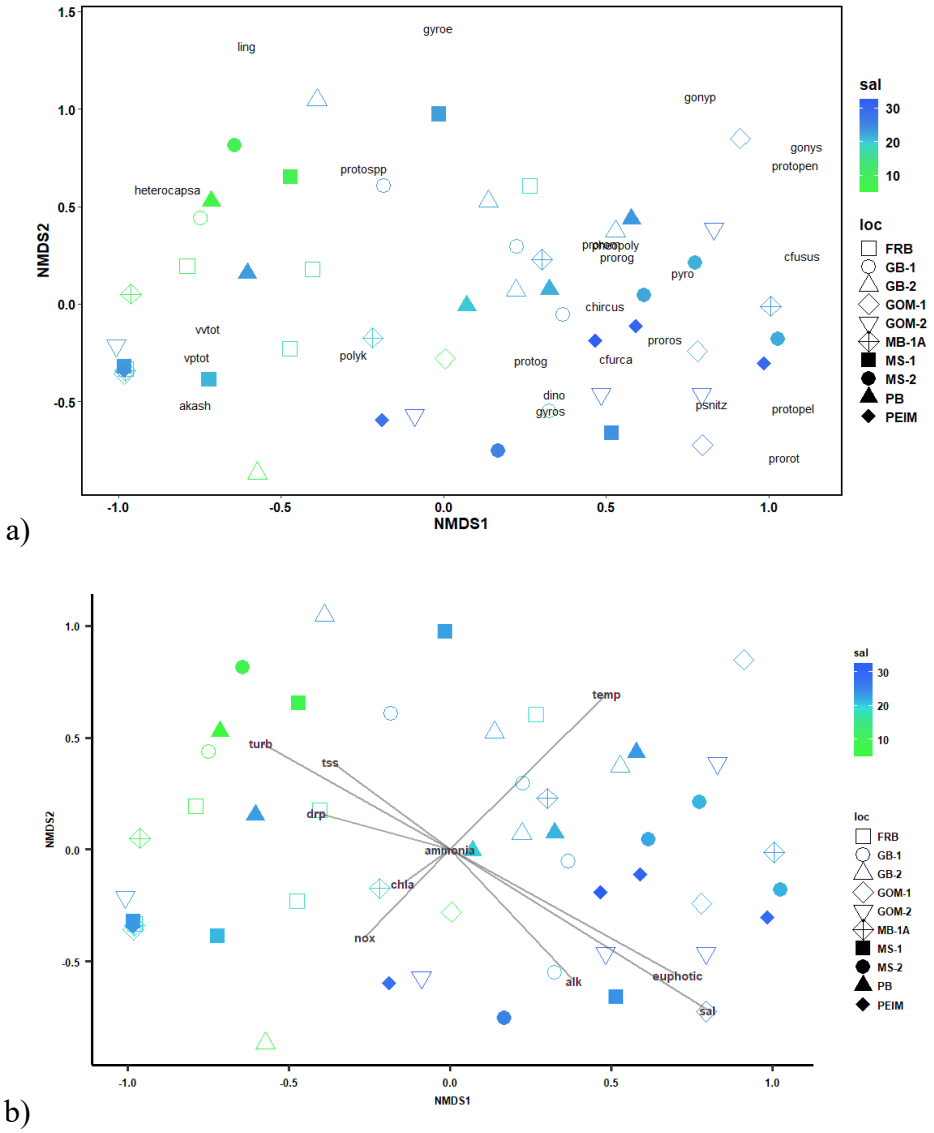

Figure 16. NMDS plots of planktonic communities in the Eastern Mississippi Sound System. **a)** NMDS plot for *Vibrio* spp. and monitored phytoplankton species. Site location is indicated by marker shape and salinity is indicated by marker color. Species abbreviations are overlain in black text. **b)** NMDS plot with structuring variables overlain as vectors. Vector length indicates the strength of the association between the variable and the observed communities. Variable names/abbreviations are printed at the end of their respective vector line segments.

CHAPTER 4 DISCUSSION

Vibrio spp. studies in the northern Gulf of Mexico often focus on vibrio population dynamics through the lens of pathogenic strains and predicting impacts on public health through shellfish vectors. This study provides a novel approach to understanding effects of physical processes and fluvial input on the abundances of *Vibrio* spp. and associated planktonic communities. Use of real-time PCR enhanced the sensitivity of the vibrio assays conducted and allowed for the enumeration of all target vibrio species, not just those easily culturable on agar. Numerous previous studies (Heidelberg et al. 2002, Randa et al. 2004, Siboni et al. 2016, Zimmerman et al. 2007) reporting water column *Vibrio* spp. population dynamics rely on samples collected from docks; however, given the proximity to man-made structure, these may not represent ambient hydrographic conditions or reflect average planktonic communities (Caine 1987). Collecting depth-integrated samples in a variety of locations ensured that samples were representative of the entire euphotic zone, not just surface waters. This sampling method was especially important in the sampling region due to the prevalence of freshwater stratification (Dzwonkowski et al. 2011, 2018).

Temperature has been previously determined as a paramount correlative factor for *Vibrio* spp. abundances (Randa et al. 2004, Motes et al. 1998, Turner et al. 2009). However, temperature was not found to be a significant correlate in our study. This is

unsurprising, as the range of temperatures in the study fell within those favorable for *Vibrio* spp. growth (Johnson et al. 2010, Wright et al. 1996, Zimmerman et al. 2007). Sampling under low temperature variability allowed us to identify other driving factors in vibrio population dynamics. Nutrients were also poor overall correlates for *Vibrio* spp. abundances, a pattern that has been reported in other estuary systems (Blackwell and Oliver 2008). NO_x had weak correlations with *Vibrio vulnificus*, and was not correlated to salinity, turbidity, or phytoplankton abundances. Past work in Mobile Bay has shown associations between sediments and nitrate nutrient fluxes which impact pelagic phytoplankton blooms; however, these interactions can be greatly affected by fluvial input patterns (Cowan et al. 1996). Alkalinity had correlations with the smallest size fraction and combined *Vibrio parahaemolyticus* abundances. Alkalinity specifically has not been studied as an environmental correlate to vibrio species, but lab-based studies have shown that alkaline-adapted *Vibrio parahaemolyticus* were more likely to survive in heat and oxidative stress conditions (Koga et al. 2002). Highest concentrations of nitrate and alkalinity were found at sites with the most marine influence (GOM-1, GOM-2, PEIM).

Although salinity, turbidity, and the E-W wind vector were identified as significant correlates in Spearman's Rank-Based Correlation analysis, they did not remain significant parameters of the LME model for either vibrio species. LME models allow for the identification of variables that drive *Vibrio* spp. variation outside of site-based variability; differences in site accounted for a large proportion of *V. parahaemolyticus* variation (41%) and nearly 100% of *V. vulnificus* variation. Therefore, significant variables identified in Spearman's correlations are likely intrinsically tied to

site. This is unsurprising, as proximity to freshwater sources/outflows and effects of the E-W wind scalar (determined by geographic location) underlie site-specific differences in favorable conditions for vibrios. Locally, the wind scalar may affect turbidity, wave action, and physical mixing potential as a function of the water column depth and the fetch length of open water that the wind can act upon; depth and fetch length varied across all sites sampled. Ammonia was retained in the models due to lack of variation (all values exceeded the upper limit of detection). Below, we explain how these fixed-effect factors may modulate *Vibrio* spp. abundances.

The interactions between meteorological, hydrographic, and biogeochemical processes in Mobile Bay and the EMSS provide a complex backdrop for understanding *Vibrio* spp. population dynamics. Due to the freshwater-dominated nature of this system, fluvial input affects an interrelated suite of hydrographic parameters (salinity, turbidity, euphotic depth, and nutrients) (Boesch et al. 2000). By reason of their effects on cellular processes (e.g., osmotic regulation, photosynthesis), salinity and turbidity regimes likely create biophysical gradients in the EMSS that structure planktonic communities (Kim et al. 2013, Lehrter et al. 1999, MacIntyre et al. 2011); the geographic extent of the gradients may be affected by meteorological factors.

4.1 Fluvial input effects on *Vibrio* spp.

In the EMSS, elevated precipitation and river flow rates are common. However, the extended duration of high river discharge in 2019, coupled with historic heavy rainfall events throughout the central and eastern US (Committee on Transportation and

Infrastructure 2019), led to extended periods of low salinity conditions in the study region (Figure 17). For example, extreme precipitation prompted the unprecedented double openings of the Bonnet Carré spillway in Lake Pontchartrain, LA. The Army Corps of Engineers opened the spillway twice in 2019: once before the sampling period (February-April) and once in the middle of the sampling period (May -July) (Figure 18). This action diverted a considerable plume of freshwater into western Mississippi Sound. Although the geographic extent of the Spillway's freshwater influence is disputed, models from the Pontchartrain Conservancy have shown that freshwater extended to the Mississippi – Alabama state line (Connor et al. 2019). The extended period of low salinity was also attributed to extensive oyster die-offs (Gledhill et al. 2020), an unusual mortality event for bottlenose dolphins (NOAA Fisheries 2020), plus a cyanobacteria bloom in coastal Mississippi which is typical for freshwater aquatic systems locally (Mississippi Department of Marine Resources 2019). Combining the effects of local and adjacent fluvial inputs, this represented an 80% increase of freshwater into the system relative to a typical year (Dzwonkowski, unpublished). Although 2019 may represent an anomalous year, the precipitation and fluvial discharge patterns observed are predicted to become more common as climate change progresses (Biasutti et al. 2012); therefore, these data may provide a glimpse into future system conditions.

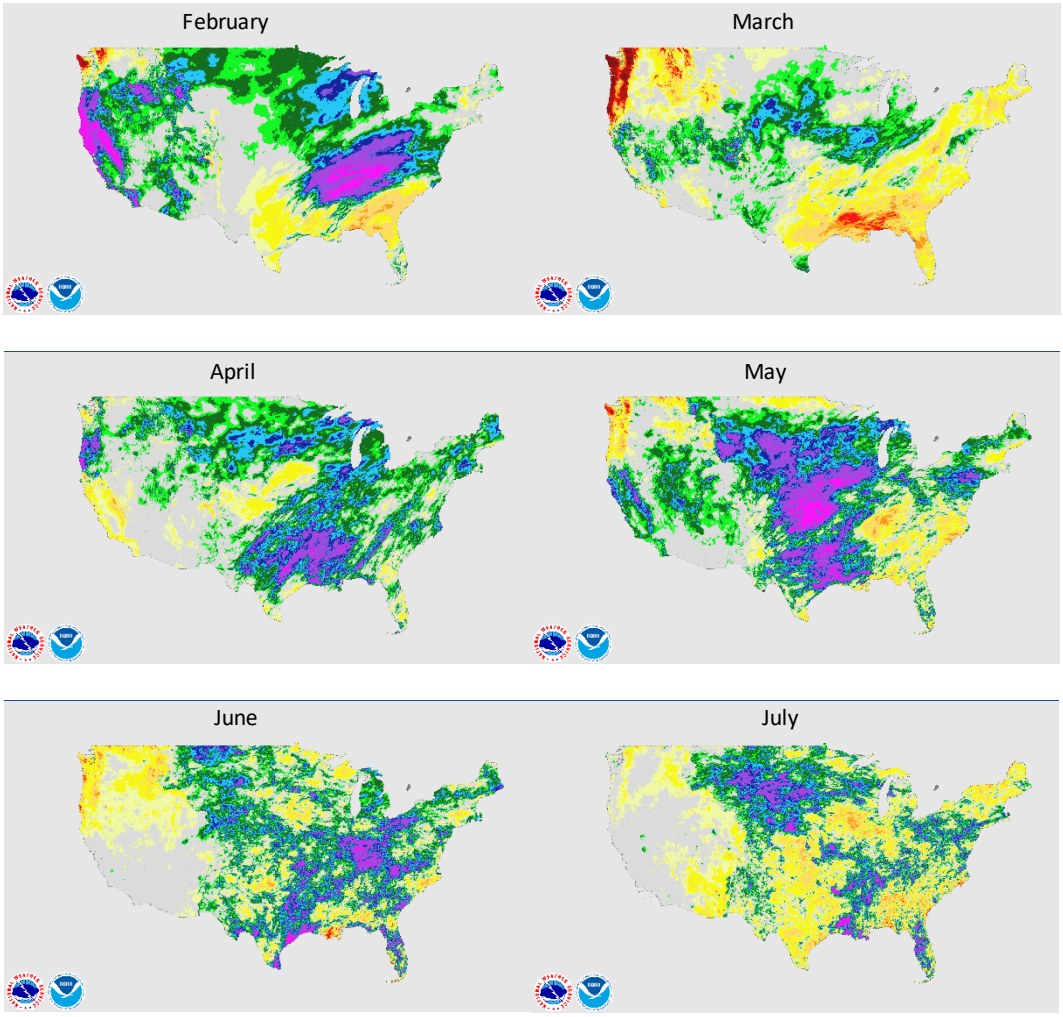

Figure 17. Monthly Precipitation Anomaly for February -July 2019. Areas in green, blue, and purple indicate zones with positive anomalous rainfall. In February, high rainfall in the Ohio Valley, one of the tributary watersheds to the Mississippi, prompted the opening of the Bonnet Carré spillway on Lake Pontchartrain. In May and June, extensive flooding and rain in the Missouri and Mississippi watersheds prompted a second opening of the spillway. Maps were accessed via the National Weather Service website (https://water.weather.gov/precip/).

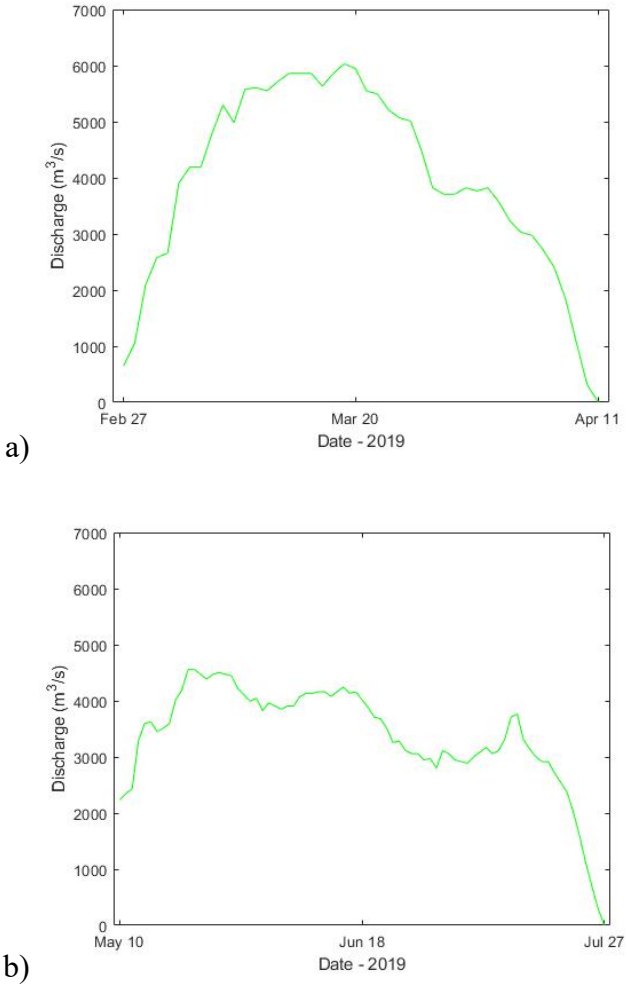

Figure 18. Freshwater discharge over the duration of the two Bonnet Carré Spillway openings in 2019. A) first opening of the Bonnet Carré Spillway. B) second opening of the Bonnet Carré Spillway. Opening the Spillway diverts water flowing in the Mississippi River away from New Orleans and into Lake Pontchartrain. From there, freshwater flows southward into the connected Lake Borgne and Mississippi Sound. Discharge data from the Army Corp of Engineers (https://www.mvn.usace.army.mil/Missions/Mississippi-River-Flood-Control/Bonnet-Carre-Spillway-Overview/Spillway-Operation-Information/)

The high influx of freshwater into the study system in 2019 had dramatic effects on regional hydrography, particularly in terms of salinity and turbidity. Salinity throughout the coastal bays and central sound sites in the EMSS remained under 15 ppt in May and June (Figure 8). This affected the structuring of biophysical gradients within the EMSS, and in turn, may have affected the abundances of *Vibrio* spp. within the sampling region. In subtropic estuaries, such as the study area, salinity can be a stronger structuring variable for *Vibrio* spp. populations than temperature (Lipp et al. 2001). Salinity correlations can even be seen in tidally dominated estuaries, like coastal Georgia (Turner et al. 2009). Low salinities in the early months of the sampling period may have provided more favorable conditions for *Vibrio vulnificus* growth throughout coastal bays and the eastern Mississippi Sound. *Vibrio vulnificus* preference for lower salinities has been demonstrated by Kelly (1982) in Galveston Bay and Randa et al. (2004) in Barnegat Bay. *Vibrio parahaemolyticus* abundances did not trend with salinity; lack of correlation with salinity can likely be attributed to the wide range of salinities that the species inhabits (Takemura et al. 2014). However, patterns with salinity are not universal. Salinity was not a significant predictor of *V. parahaemolyticus* in water when compared across sites in Washington, the northern Gulf of Mexico and Maryland (Johnson et al. 2012), implying some regional specificity of environmental predictors for *Vibrio* spp. Local variability of vibrio population dynamics in response to environmental variables has been demonstrated by Nash (2018) with *Vibrio cholerae* in Mobile Bay and by Johnson et al.(2010) with pathogenic *V. vulnificus* and *V. parahaemolyticus* in the Mississippi Sound System.

Abundances of both vibrio species positively correlated with turbidity; trends previously demonstrated locally by Zimmerman et al. (2007) and Johnson et al. (2010), and in North Carolina estuaries by Blackwell and Oliver (2008). Turbidity is mostly caused by resuspension of sediment particles into the water column but can also have biological or detrital components. Sediments have been shown to be an important reservoir of vibrios. Johnson et al. (2010) suggest that *Vibrio parahaemolyticus* has a particular affinity for sequestering in the sediment. *Vibrio vulnificus* has also been isolated from sediments, but not at consistently high concentrations across past studies (Johnson et al. 2010, Vanoy et al. 1992, Williams and LaRock 1985). The complex sediment environment may offer protection from grazers (e.g., protists) and provide compounds for cellular growth (e.g. dissolved organic matter); similar advantages may be gained through attachment onto surfaces (pelagic or benthic), especially chitinous material (e.g. metazoans, diatom chain filaments; Johnson et al. 2010, Takemura et al. 2014). Sediment resuspension thus represents a pathway for the reintroduction of vibrios into the water column, where they can interact with components of the microbial loop, colonize planktonic substrate, and be consumed by higher trophic level organisms.

On average, *Vibrio parahaemolyticus* abundances were greatest at FRB, MB-1A, and PEIM, despite these sites having very different salinity and turbidity regimes. High *Vibrio parahaemolyticus* abundances were found at FRB and MB-1A when turbidity was higher than 10 NTU. We hypothesize that the high abundances at these sites may represent two distinct lifestyles of *Vibrio parahaemolyticus*: those that sequester in sediments (and are occasionally resuspended) and those associated with pelagic plankton responding to fluvial input. Differences in lifestyle are also accompanied by different

physiology in terms of location and motility of flagella (Belas et al. 1986, McCarter 2001). Free-living vibrios tend to have a polar flagellum specialized for movement in the water column (Belas et al. 1986). Particle or sediment associated vibrios have greater presence of lateral flagella and pili that aid in attachment and movement along solid surfaces. Additionally, Belas and Colwell (1982) demonstrated that environmental factors like salinity can affect the expression of the flagellar phenotypes associated with surface-colonizing *Vibrio parahaemolyticus*. This suggests a complex interaction between salinity and sediment resuspension in controlling amounts of *Vibrio* spp. bacteria in the water column. Because salinity and turbidity are linked in this system, fluvial input into the EMSS likely affects vibrio levels through various mechanisms (lowering salinity, resuspending sediment, affecting expression of flagellar phenotypes) that impact distinct reservoirs of *Vibrio* spp.

4.2 Meteorological effects on *Vibrio* spp.

Aside from freshwater input, results from our study suggest the emerging importance of wind as a predictor/ environmental correlate for *Vibrio* spp. abundances. South winds have historically prevailed in the region, evidenced in Zimmerman et al. 2007. In the EMSS, winds moving from the west to the east can promote regional upwelling by causing surface waters to move offshore via Ekman transport (Figure 19a). Winds moving from the east to the west promotes regional downwelling by pushing surface waters towards the shoreline (Figure 19b). Schroeder and Wiseman (1986) showed that even short-duration (24-48 hour) wind events can promote upwelling and

downwelling processes. Both *Vibrio vulnificus* and *Vibrio parahaemolyticus* abundances were negatively correlated to the E-W wind vector. West originating winds were notated as a negative vector, whereas east originating winds were notated as a positive vector; therefore, *Vibrio* spp. abundances decreased with East winds. This phenomenon could be attributed to advective processes (salinity increasing due to influx of marine water at the surface) or reduction in sediment resuspension from local downwelling.

Figure 19. Wind-driven upwelling and downwelling schematics for the Eastern Mississippi Sound System. a) West Wind Scenario: these conditions favor the formation of a local upwelling zone. The panel on the left shows wind direction through the sample region and the panel on the right shows a slice through the water column to illustrate the interactions between wind and water movement. The circle with a dot in the middle indicates wind and water movement out of the page. Although surface currents are parallel to the wind, net water transport moves 90 degrees to the right of the direction of wind forcing (Ekman transport), pushing water offshore. The difference in surface water height is denoted by the light blue dashed line. b) East Wind Scenario: these conditions favor the formation of a local downwelling zone. The panel on the left shows wind direction through the sample region and the panel on the right shows a slice through the water column to illustrate the interactions between wind and water movement. The circle with an x in the middle indicates wind and water movement into the page. Although surface currents are parallel to the wind, net water transport moves 90 degrees to the right of the direction of wind forcing (Ekman transport), pushing water towards the shore. The difference in surface water height is denoted by the light blue dashed line.

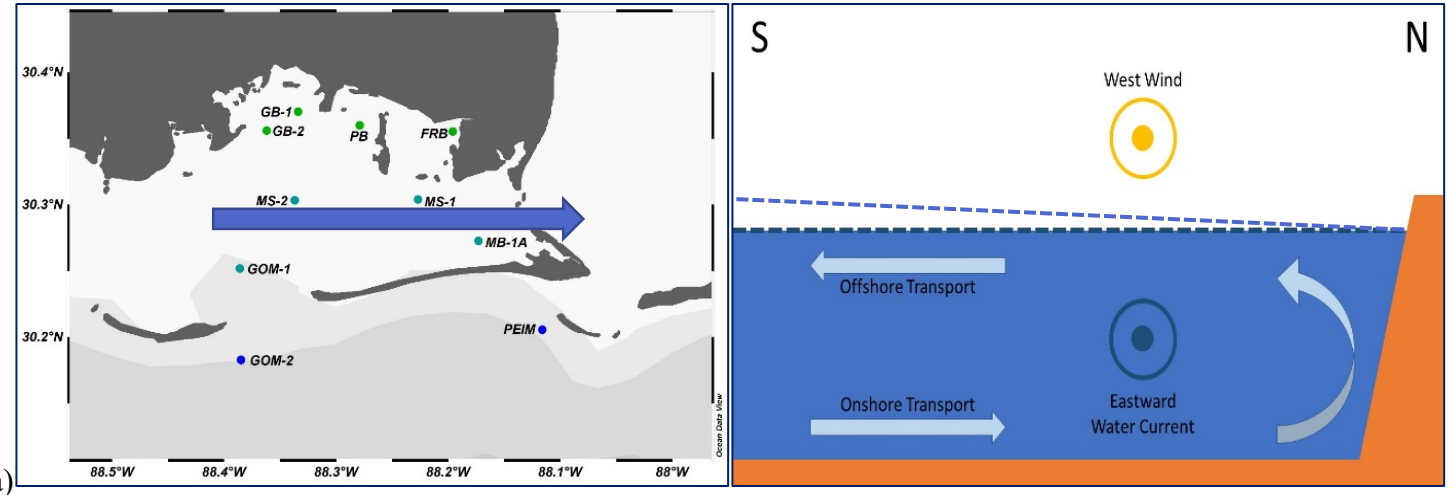
30.4°N
30.3°N
30.2°N
GB-1
GB-2
PB
FRB
MS-2
MS-1
MB-1A
GOM-1
PEIM
GOM-2
88.5°W
88.4°W
88.3°W
88.2°W
88.1°W
88°W
S
N
West Wind
Offshore Transport
Onshore Transport
Eastward
Water Current

a)

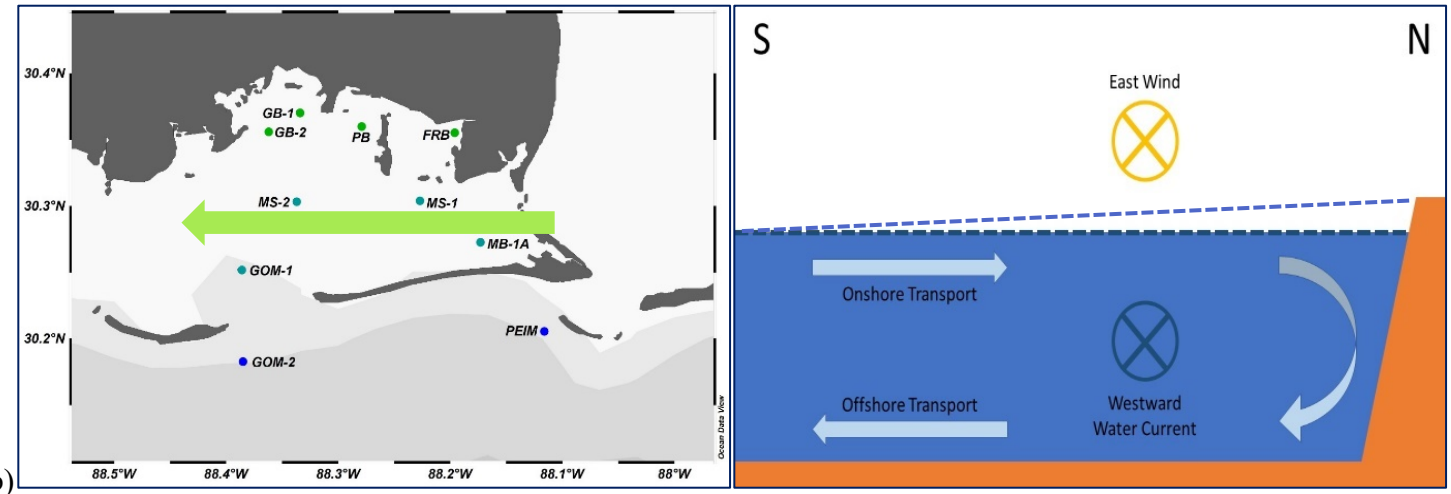
30.4°N
30.3°N
30.2°N
GB-1
GB-2
PB
FRB
MS-2
MS-1
MB-1A
GOM-1
PEIM
GOM-2
88.5°W
88.4°W
88.3°W
88.2°W
88.1°W
88°W
S
N
East Wind
Onshore Transport
Offshore Transport
Westward
Water Current

b)

The duration of these wind events may affect the strength of the vibrio correlation. Our data suggests that even short-term wind vector patterns (1 to 24 hours prior to sampling) may be useful metrics for predicting *Vibrio* spp. abundances in the EMSS. It is also important to note that wind is a unique forcing mechanism that can affect the expanse of freshwater input influence; wind speed and direction can have indirect effects on salinity, turbidity, and other factors involved in structuring biophysical gradients in the study region (Coogan and Dzwonkowski 2018, Du et al. 2018, Kim and Park 2012, Kim et al. 2013).

4.3 *Vibrio* spp. and harmful algae

Fluvial input not only impacts the population dynamics of vibrio themselves, but also the planktonic communities that they inhabit. Earlier research has shown that vibrios readily associate with zooplankton (Colwell 1996, Huq et al. 1996, Montanari et al. 1999, Turner et al. 2009) but these relationships are poorly understood in the Northern Gulf of Mexico. Size-specific interactions have also not been studied for this region. Results from our study suggest associations with numerically rare harmful algal species (actively monitored), and neither *Vibrio* spp. nor these harmful species correlated with metrics of the bulk phytoplankton (i.e., chlorophyll a). The lack of correlation indicates that these harmful algal species are not the main drivers of chlorophyll signals in this region, and/or that there is a considerable detrital chlorophyll signal in the EMSS. The lack of correlation undermines the validity of using chlorophyll a as a predictive metric for *Vibrio* spp. in this region, especially in seasons with limited temperature variation. Past

studies in the northern Gulf of Mexico similarly did not find significant relationships between *Vibrio* spp. and chlorophyll a (Johnson et al. 2012 and Zimmerman et al. 2007) but studies in other estuarine systems have (Barnegat Bay, NJ- Randa et al. 2004, Venetian Lagoon, Italy -Caburlotto et al. 2010, Great Bay, NH - Urquhart et al. 2016). Therefore, bulk chlorophyll a is likely a regionally specific variable for vibrio correlation that may be confounded by other physical or hydrographic factors.

In our study sites, 30-50% of target vibrios associated with particles larger than 5 microns. Monitored phytoplankton groups varied in size from 2 – 230 μm (Table 10), meaning that there is a diversity in the size of biological particles available for *Vibrio* spp. to associate with in the EMSS. Fluvial sediment particles also vary in size, from clay grains (~2 μm) to sand (up to 1 mm). Detrital particles can be even larger, and *Vibrio* spp. may colonize these surfaces as a biofilm (Yildiz and Visick 2009). Vibrio-particle interactions were investigated by Hsieh et al. (2007) in estuaries of North Carolina; increased particulates in the water column (3- 60 μm, attributed to phytoplankton) were associated with an increase in *Vibrio* spp. abundance associated with particles. Frequency of particle association also decreased with increasing salinity. Although *Vibrio* spp. interactions with specific particle size groupings were not isolated in Hsieh et al. 2007, an opposite trend between salinity and *Vibrio vulnificus* particle size association was seen in this study (Table 14a).

Table 10. Size ranges and HAB status of identified phytoplankton species. The last column on the right indicates which filter size members of this species or genus would likely be caught on in the sequential filtration method outlined in this study. Green highlighted species are those which had significant positive correlations with vibrio abundances. Blue highlighted species are those which had significant negative correlations with vibrio abundances.

Species	Type	Size (µm)	HAB/toxin producer?	Caught on filter
Gyrodinium estuariale	dinoflagellate	9-16		5 µm
Karlodinium veneficum	dinoflagellate	7-18	X	5 µm
Prorocentrum triestinum	dinoflagellate	6-22		5 µm
Ceratium furca	dinoflagellate	30-230	X	35 µm / 5 µm
Ceratium fusus	dinoflagellate	30-231	X	35 µm / 5 µm
Ceratium hircus	dinoflagellate	32-200		35 µm / 5 µm
Diplopsalis lenticula	dinoflagellate	25-70		35 µm / 5 µm
Gonyaulax polygramma	dinoflagellate	26-66		35 µm / 5 µm
Gonyaulax spinifera	dinoflagellate	25-140	X	35 µm / 5 µm
Gyrodinium spirale	dinoflagellate	20-105		35 µm / 5 µm
Heterocapsa spp.	dinoflagellate	9-30		35 µm / 5 µm
Prorocentrum gracile	dinoflagellate	25-55		35 µm / 5 µm
Prorocentrum micans	dinoflagellate	20-75	X	35 µm / 5 µm
Prorocentrum scutellum	dinoflagellate	34-45		35 µm / 5 µm
Protoperidinium quinquecorne	dinoflagellate	30-40		35 µm / 5 µm
Pseudo-nitzschia spp.	diatom	2-175	X	35 µm / 5 µm
Pyrodinium bahamense	dinoflagellate	33-52		35 µm / 5 µm
Pyrophacus horologium	dinoflagellate	30-120		35 µm / 5 µm
Akashiwo sanguinea	dinoflagellate	40-80	X	35 µm
Brachydinium capitatum	dinoflagellate	95-123		35 µm
Dinophysis caudata	dinoflagellate	43-94	X	35 µm
Katodinium glaucum	dinoflagellate	36-62		35 µm
Lingulodinium polyedrum	dinoflagellate	40-60	X	35 µm
Pheopolykrikos hartmanii	dinoflagellate	40-65		35 µm
Polykrikos kofoidii	dinoflagellate	60-160		35 µm
Prorocentrum concavum	dinoflagellate	38-55		35 µm
Prorocentrum emarginatum	dinoflagellate	35-42		35 µm
Protoperidinium grande	dinoflagellate	65-100		35 µm
Protoperidinium pallidum	dinoflagellate	65-100		35 µm
Protoperidinium pellucidum	dinoflagellate	35-52		35 µm
Protoperidinium pentagonum	dinoflagellate	60-80		35 µm
Protoperidinium spp.	dinoflagellate	40-70		35 µm
Protoperidinium steidingerae	dinoflagellate	65-130		35 µm

In this study, *Vibrio vulnificus* associated with smaller particles in low salinity, suggesting some role for freshwater input in determining particle association. The median salinity when the majority of *V. vulnificus* in a sample associated with particles ≤ 5 µm (11 ppt) was significantly different from the median salinity when the majority of *V. vulnificus* in a sample associated with particles ≥ 5 µm (22 ppt). Given that *Vibrio vulnificus* preferred salinities are low (Table 1), associating with large particles in high salinity may offer potential protection from osmotic stress due to the availability of leaky osmolytes (Morris et al. 2012), as well as protection from consumption and proximity to cellular exudates for food. Conversely, *Vibrio parahaemolyticus* did not appear to show a differential particle size preference; however, *V. parahaemolyticus* was associated with large particles over a greater range of salinities than *V. vulnificus*. Kaneko and Colwell (1975) demonstrated that *V. parahaemolyticus* more readily associated with copepods in lower (2 ppt) salinities (compared to brackish, 16 ppt) and that adherence to chitin-based organisms may offer protection from thermal and osmotic stressors. Our data suggest that during 2019, *V. vulnificus* may have used particle associations to better adapt to environmental conditions (i.e., higher salinities) not favorable for their growth while *V. parahaemolyticus* may be better adapted among the range of salinities observed (i.e. as to not consistently require associations with larger particles). The size of particles that vibrios associate with can have notable implications for retaining these bacteria in microbial loop processes (e.g., viral lysis, ingestion by microzooplankton) or potentially shunting them to higher trophic levels via ingestion by larger organisms (e.g. oysters, crabs, fish) (DePaola et al. 1994).

Although vibrios in the <5 μm size fraction could be free living, it is possible that these cells are still particle associated. Protists and other nanoplankton were not identified in this study but may be an understudied reservoir for vibrio attachment. Asplund et al. (2011) showed that ciliates may be important biotic correlates and controls for *Vibrio* spp. populations in coastal India, but these relationships have yet to be studied in the northern Gulf of Mexico. Larger zooplankton were not enumerated for this study, but among those visually identified on filters were copepods, barnacle nauplii, chaetognaths, larval fish, and decapod zoea.

In addition to particle-size associations, correlations between combined *Vibrio* spp. Levels and specific phytoplankton groups were identified. *Vibrio vulnificus* abundances were positively correlated to low salinity-preferring phytoplankton (*Akashiwo sanguinea* and *Heterocapsa* spp) and were negatively correlated to species with higher salinity tolerances (*Prorocentrum* spp. and *Pseudo-nitzschia* spp.). *Vibrio parahaemolyticus* was only negatively correlated with *Pseudo-nitzschia* spp. diatoms. It is important to note that these correlations are only describing environmental associations, not necessarily physical attachments. Therefore, positive correlations can be used to indicate environmental conditions where both species thrive. In PERMANOVA-NMDS analysis, communities characterized by the presence of *A. sanguinea* and *Heterocapsa* spp. were driven by low salinity, shallow euphotic depth, and higher turbidity, whereas communities dominated by *Pseudo-nitzschia* spp were driven by high salinity, deep euphotic zone, and low turbidity.

4.4 Regional recommendations for future monitoring of *Vibrio* spp.

By elucidating the complex interactions between meteorological, hydrographic, and biogeochemical processes that underlie *Vibrio* spp. abundances in this region, data collected may inform the next iteration of *Vibrio* spp. risk assessment models (FDA CFSAN 2005, FAO & WHO 2020, Jacobs et al. 2010).

The current vibrio model used for the northern Gulf of Mexico (GOM) predicts *Vibrio parahaemolyticus* concentrations in oyster tissue. This model, developed by the US Food and Drug Administration - Center for Food Safety and Applied Nutrition, is based on a complete risk assessment from 2005. Although this model is successful in predicting vibrio risk associated with shellfish, additional modelling efforts are needed to predict water-borne *Vibrio* spp. risk in the EMSS. Additionally, there are no current models for *Vibrio vulnificus*, either free living or oyster associated, for the northern GOM. The United States National Oceanographic and Atmospheric Administration (NOAA) has developed a waterborne *Vibrio vulnificus* model for the Chesapeake Bay, ground-truthed by years of in-situ data collection, but this model predicts probability of presence, not abundance (Jacobs et al. 2010). Our study provides data that can be used to model *Vibrio parahaemolyticus* and *Vibrio vulnificus* abundances in the water column. Novel physical and biological correlates identified in this study may also be useful parameters to include in future iterations of vibrio modelling for this region.

In-situ biogeochemical monitoring of sites in the EMSS are only conducted by state environmental agencies once every three years. Given that most shellfish aquaculture for the state of Alabama occurs in this region (Gregalis et al. 2008), and that environmental conditions can vary dramatically in this estuary system, more frequent

sampling may provide stakeholders with better information regarding potential conditions favoring *Vibrio* spp. abundance increases. Continuous meteorology and hydrography monitoring stations exist on the far eastern portions of the study region (Dauphin Island and Cedar Point ARCOS stations), but no continuous monitoring efforts exist for sites in Portersville Bay or Grand Bay, AL. These sites are the predominant zones of active off-bottom oyster aquaculture in Alabama. The addition of a continuous (or semi-continuous) monitoring station like others in the ARCOS network, combined with increased biogeochemical monitoring, could provide an information framework to support additional off-bottom culture development in this zone.

Correlations between certain phytoplankton groups and *Vibrio* spp. abundance highlight the potential for synergy between agencies that monitor for harmful algal blooms (HABs) and stakeholders directly affected by vibrio levels (i.e., oyster farmers and commercial fishermen). Phytoplankton species enumerated in this study are among those regularly monitored for, and thus, regularly encountered as potentially harmful bloom forming species in the EMSS. Detections of species positively correlated with *Vibrio* spp. may be useful for state agencies in leveraging their existing monitoring programs; high concentrations of these species could serve as an early warning/ alert tool for additional bacteriological sampling. The described tool in and of itself does not constitute a regulatory action but utilizing this framework for interagency collaboration may aid in efficiency of in-situ vibrio risk assessment for the region. Phytoplankton data collected by state monitoring agencies could be relayed to oyster farmers and commercial fishermen, who can then make informed decisions about harvest and handling procedures if an enhanced vibrio risk is indicated. Local extension partners like the Auburn

University Shellfish Lab may help to facilitate these communication streams between stakeholders and state agencies. The proposed partnerships can further support economic development of off-bottom oyster resources while aiming to mitigate risk to stakeholders who are directly affected by *Vibrio* spp. abundances.

4.5 Future Implications

Climate models for the Gulf of Mexico region show that extreme precipitation events are predicted to increase along the Gulf Coast moving into later decades of the 21st century (Biasutti et al. 2012). As the climate warms, the hydrological cycle intensifies, leading to more intense convective cells and precipitation events (Karl and Knight 1998). Greater rainfall in coastal areas and in river basins draining to the Northern Gulf of Mexico will likely impact duration of low salinity waters in estuarine margins.

As coastal flooding becomes more frequent with climate change, conditions favorable for the proliferation of planktonic *Vibrio vulnificus* are likely to become more common. Coastal planktonic communities will likely shift to low-salinity and high-turbidity tolerant species, with greater potential for blooms of freshwater taxa like cyanobacteria (e.g. as observed in western Mississippi Sound during 2019). Low salinities also affect vibrio- particle interactions and results from our study suggest that *Vibrio vulnificus* will associate with smaller particles in these conditions. This has implications for increased assimilation of *Vibrio* spp. into oysters and other filter feeding organisms. Larval oysters have been shown to derive up to 60% of their food from particles between 0.5 and 10 microns (Baldwin and Newell 1995) and adult oysters can concentrate bacterioplankton

in their tissues by nearly 100-fold relative to ambient levels in the water column. By associating primarily with smaller particles in near-shore localities, the amount of *Vibrio vulnificus* directly ingested by higher trophic level organisms may be reduced. Conversely, if *Vibrio parahaemolyticus* associates with larger particles (e.g., chitinous) in low salinities to adapt to stressful osmotic conditions (Kaneko and Colwell 1975), they may be more easily consumed by larger predators (fish, blue crabs, shrimp) and assimilated into gut microbiota. Environmental changes can affect the abundance and assemblage of *Vibrio* spp. in certain reservoirs, ultimately affecting which vector contains the greatest vibrio risk.

REFERENCES

Alabama Department of Environmental Management, 2016. Alabama's Water Quality Assessment and Listing Methodology. SOPs 2041, 2042, 2044, 2046, 2047, 2061, 2062, 2063, and 9021; procedures can be requested at http://adem.alabama.gov/programs/water/waterquality.cnt.

Army Corps of Engineers., 2019. https://www.mvn.usace.army.mil/Missions/Mississippi-River-Flood-Control/Bonnet-Carre-Spillway-Overview/Spillway-Operation-Information/

Asplund, M.E., Rehnstam-Holm, A.S., Atnur, V., Raghunath, P., Saravanan, V., Härnström, K., Collin, B., Karunasagar, I. and Godhe, A., 2011. Water column dynamics of Vibrio in relation to phytoplankton community composition and environmental conditions in a tropical coastal area. *Environmental Microbiology*, *13*(10), pp.2738-2751.

Baldwin, B.S. and Newell, R.I., 1995. Relative importance of different size food particles in the natural diet of oyster larvae. *Marine Ecology Progress Series*, *120*, pp.135-145.

Belas, M.R. and Colwell, R.R., 1982. Adsorption kinetics of laterally and polarly flagellated Vibrio. *Journal of Bacteriology*, *151*(3), pp.1568-1580.

Belas, R., Simon, M., and Silverman, M., 1986. Regulation of lateral flagella gene transcription in Vibrio parahaemolyticus. *Journal of Bacteriology*, *167*(1), pp.210-218.

Bell, W. and Mitchell, R., 1972. Chemotactic and growth responses of marine bacteria to algal extracellular products. *The Biological Bulletin*, *143*(2), pp.265-277.

Biasutti, M., Sobel, A.H., Camargo, S.J. and Creyts, T.T., 2012. Projected changes in the physical climate of the Gulf Coast and Caribbean. *Climatic Change*, *112*(3), pp.819-845.

Blackwell, K.D. and Oliver, J.D., 2008. The ecology of Vibrio vulnificus, Vibrio cholerae, and Vibrio parahaemolyticus in North Carolina estuaries. *The Journal of Microbiology*, *46*(2), pp.146-153.

Blodgett, R., 2020. Bacteriological Analytical Manual - BAM Appendix 2: Most Probable Number from Serial Dilution. Food and Drug Administration. Accessed at https://www.fda.gov/food/laboratory-methods-food/bam-appendix-2-most-probable-number-serial-dilutions.

Boesch, D.F., Field, J.C. and Scavia, D. eds., 2000. *The potential consequences of climate variability and change on coastal areas and marine resources: Report of the Coastal Areas and Marine Resources Sector Team, US National Assessment of the Potential Consequences of Climate Variability and Change, US Global Change Research Program* (No. 21). US Department of Commerce, National Oceanic and Atmospheric Administration, National Ocean Service, National Centers for Coastal Ocean Science, Coastal Ocean Program.

Caburlotto, G., Haley, B.J., Lleò, M.M., Huq, A. and Colwell, R.R., 2010. Serodiversity and ecological distribution of Vibrio parahaemolyticus in the Venetian Lagoon, Northeast Italy. *Environmental Microbiology Reports*, *2*(1), pp.151-157.

Caine, E.A., 1987. Potential effect of floating dock communities on a South Carolina estuary. *Journal of Experimental Marine Biology and Ecology*, *108*(1), pp.83-91.

Campbell, M.S. and Wright, A.C., 2003. Real-time PCR analysis of Vibrio vulnificus from oysters. *Applied and Environmental Microbiology*, *69*(12), pp.7137-7144.

Center for Disease Control and Prevention., 2018. Vibrio Species Causing Vibriosis. Available at: https://www.cdc.gov/vibrio/index.html. Last accessed: September 10, 2019.

Chart, H., 2012. 30 - Vibrio, mobiluncus, gardnerella and spirillum: Cholera; vaginosis; rat bite fever, Editor(s): David Greenwood, Mike Barer, Richard Slack, Will Irving, Medical Microbiology (Eighteenth Edition), Churchill Livingstone, Pages 314-323, ISBN 9780702040894, https://doi.org/10.1016/B978-0-7020-4089-4.00045-7. (http://www.sciencedirect.com/science/article/pii/B9780702040894000457)

Colwell, R.R., 1996. Global climate and infectious disease: the cholera paradigm. *Science, 274*(5295), pp.2025-2031.

Committee on Transportation and Infrastructure., 2019. Concepts for the next Water Resources Development Act: promoting resiliency of our nation's water resources infrastructure. Hearing before the Subcommittee on Water Resources and Environment of the Committee on Transportation and Infrastructure, House of Representatives, One Hundred Sixteenth Congress, first session, November 19, 2019. Washington D.C.; Staff, Subcommittee on Water Resources and Environment. Accessed via: https://www.congress.gov/116/meeting/house/110195/documents/HHRG-116-PW02-20191119-SD001.pdf

Connor, P.F., Lopez, J., Henkel, T., Hillmann, E., Hopkins, M., Baker, D., Butcher, K., DeSantiago, K., and Songy, A., 2019. Hydrocoast Salinity Map: May 27 - June 02, 2019 [map], 1:1,100,000, Lake Pontchartrain Basin Foundation , N.O., La.

Coogan, J. and Dzwonkowski, B., 2018. Observations of wind forcing effects on estuary length and salinity flux in a river-dominated, microtidal estuary, Mobile Bay, Alabama. *Journal of Physical Oceanography*, *48*(8), pp.1787-1802.

Cowan, J.L., Pennock, J.R. and Boynton, W.R., 1996. Seasonal and interannual patterns of sediment-water nutrient and oxygen fluxes in Mobile Bay, Alabama (USA): regulating factors and ecological significance. *Marine Ecology Progress Series*, *141*, pp.229-245.

Davis, B.J., Jacobs, J.M., Zaitchik, B., DePaola, A. and Curriero, F.C., 2019. Vibrio parahaemolyticus in the Chesapeake Bay: operational in situ prediction and forecast models can benefit from inclusion of lagged water quality measurements. *Applied and Environmental Microbiology*, *85*(17), pp. e01007-19.

De Magny, G.C., Murtugudde, R., Sapiano, M.R., Nizam, A., Brown, C.W., Busalacchi, A.J., Yunus, M., Nair, G.B., Gil, A.I., Lanata, C.F. and Calkins, J., 2008. Environmental signatures associated with cholera epidemics. *Proceedings of the National Academy of Sciences*, *105*(46), pp.17676-17681.

DePaola, A., Capers, G.M. and Alexander, D., 1994. Densities of Vibrio vulnificus in the intestines of fish from the US Gulf Coast. *Applied and Environmental Microbiology*, *60*(3), pp.984-988.

DePaola, A., Nordstrom, J.L., Bowers, J.C., Wells, J.G. and Cook, D.W., 2003. Seasonal abundance of total and pathogenic Vibrio parahaemolyticus in Alabama oysters. *Applied and Environmental Microbiology*, *69*(3), pp.1521-1526.

Du, J., Park, K., Shen, J., Dzwonkowski, B., Yu, X. and Yoon, B.I., 2018. Role of baroclinic processes on flushing characteristics in a highly stratified estuarine system, Mobile Bay, Alabama. *Journal of Geophysical Research: Oceans*, *123*(7), pp.4518-4537.

Dzwonkowski, B., Park, K., Ha, H.K., Graham, W.M., Hernandez, F.J. and Powers, S.P., 2011. Hydrographic variability on a coastal shelf directly influenced by estuarine outflow. *Continental Shelf Research*, *31*(9), pp.939-950

.

Dzwonkowski B, Park K, Collini R., 2015. The coupled estuarine-shelf response of a river-dominated system during the transition from low to high discharge. *Journal of Geophysical Research: Oceans* 120:6145–6163

Dzwonkowski, B., Fournier, S., Park, K., Dykstra, S.L. and Reager, J.T., 2018. Water column stability and the role of velocity shear on a seasonally stratified shelf, Mississippi Bight, Northern Gulf of Mexico. *Journal of Geophysical Research: Oceans*, *123*(8), pp.5777-5796.

FDA Center for Food Safety and Applied Nutrition., 2005. Quantitative risk assessment on the public health impact of pathogenic Vibrio parahaemolyticus in raw oysters. https://www.fda.gov/food/cfsan-risk-safety-assessments/quantitative-risk-assessment-public-health-impact-pathogenic-vibrio-parahaemolyticus-raw-oysters. Accessed July 6, 2021.

Food and Agriculture Organization of the United Nations & World Health Organization., 2020. Risk assessment tools for Vibrio parahaemolyticus and Vibrio vulnificus associated with seafood. Food and Agriculture Organization of the United Nations. https://apps.who.int/iris/handle/10665/330867. License: CC BY-NC-SA 3.0 IGO

Gelfenbaum, G. and Stumpf. R.P., 1993. Observations of currents and structure across a buoyant plume front density. *Estuaries* 16:40–52

Gilbert, J.A., Steele, J.A., Caporaso, J.G., Steinbrück, L., Reeder, J., Temperton, B., Huse, S., McHardy, A.C., Knight, R., Joint, I. and Somerfield, P., 2012. Defining seasonal marine microbial community dynamics. *The ISME Journal*, *6*(2), pp.298-308.

Givens, C.E., Bowers, J.C., DePaola, A., Hollibaugh, J.T. and Jones, J.L., 2014. Occurrence and distribution of Vibrio vulnificus and Vibrio parahaemolyticus–potential roles for fish, oyster, sediment and water. *Letters in Applied Microbiology*, *58*(6), pp.503-510.

Gledhill, J.H., Barnett, A.F., Slattery, M., Willett, K.L., Easson, G.L., Otts, S.S. and Gochfeld, D.J., 2020. Mass Mortality of the Eastern Oyster Crassostrea virginica in the Western Mississippi Sound Following Unprecedented Mississippi River Flooding in 2019. *Journal of Shellfish Research*, *39*(2), pp.235-244.

Greenfield, D.I., Gooch Moore, J., Stewart, J.R., Hilborn, E.D., George, B.J., Li, Q., Dickerson, J., Keppler, C.K. and Sandifer, P.A., 2017. Temporal and environmental factors driving Vibrio vulnificus and V. parahaemolyticus populations and their associations with harmful algal blooms in South Carolina detention ponds and receiving tidal creeks. *GeoHealth*, *1*(9), pp.306-317.

Gregalis, K.C., Powers, S.P. and Heck, K.L., 2008. Restoration of oyster reefs along a bio-physical gradient in Mobile Bay, Alabama. *Journal of Shellfish Research*, *27*(5), pp.1163-1169.

Harriague, A.C., Di Brino, M., Zampini, M., Albertelli, G., Pruzzo, C. and Misic, C., 2008. Vibrios in association with sedimentary crustaceans in three beaches of the northern Adriatic Sea (Italy). *Marine Pollution Bulletin*, *56*(3), pp.574-579.

Heidelberg, J.F., Heidelberg, K.B. and Colwell, R.R., 2002. Seasonality of Chesapeake Bay bacterioplankton species. *Applied and Environmental Microbiology*, *68*(11), pp.5488-5497.

Holiday, D., Carter, G., Gould, R.W. and MacIntyre, H., 2007. Harmful Algal Blooms in the Mississippi Sound and Mobile Bay: Using MODIS Aqua and In Situ Data for HABs in the Northern Gulf of Mexico (No. NRL/PP/7330-07-7181). Naval Research Lab Washington DC.

Holiday, D.M., 2009. Remote sensing of harmful algal blooms in the Mississippi Sound and Mobile Bay: Modelling and algorithm formation. *Dissertations*. 1085. https://aquila.usm.edu/dissertations/1085

Hsieh, J.L., Fries, J.S. and Noble, R.T., 2007. Vibrio and phytoplankton dynamics during the summer of 2004 in a eutrophying estuary. *Ecological Applications*, *17*(sp5), pp. S102-S109.

Huq, A., Xu, B., Chowdhury, M.A., Islam, M.S., Montilla, R. and Colwell, R.R., 1996. A simple filtration method to remove plankton-associated Vibrio cholerae in raw water supplies in developing countries. *Applied and Environmental Microbiology*, *62*(7), pp.2508-2512.

Huq, A., Small, E.B., West, P.A., Huq, M.I., Rahman, R. and Colwell, R.R., 1983. Ecological relationships between Vibrio cholerae and planktonic crustacean copepods. *Applied and Environmental Microbiology*, *45*(1), pp.275-283

Jacobs, J.M., Rhodes, M.M.R., Brown, C.W., Hood, R.R., Leight, A., Long, W. and Wood, R., 2010. Predicting the distribution of Vibrio vulnificus in Chesapeake Bay.

Johnson, C.N., Flowers, A.R., Noriea III, N.F., Zimmerman, A.M., Bowers, J.C., DePaola, A. and Grimes, D.J., 2010. Relationships between environmental factors and pathogenic vibrios in the northern Gulf of Mexico. *Applied and Environmental Microbiology*, *76*(21), pp.7076-7084.

Johnson, C.N., Bowers, J.C., Griffitt, K.J., Molina, V., Clostio, R.W., Pei, S., Laws, E., Paranjpye, R.N., Strom, M.S., Chen, A. and Hasan, N.A., 2012. Ecology of Vibrio parahaemolyticus and Vibrio vulnificus in the coastal and estuarine waters of Louisiana, Maryland, Mississippi, and Washington (United States). *Applied and Environmental Microbiology*, *78*(20), pp.7249-7257.

Kaneko, T. and Colwell, R.R., 1975. Adsorption of Vibrio parahaemolyticus onto chitin and copepods. *Applied Microbiology*, *29*(2), pp.269-274.

Karl, T.R. and Knight, R.W., 1998. Secular trends of precipitation amount, frequency, and intensity in the United States. *Bulletin of the American Meteorological Society*, *79*(2), pp.231-242.

Kelly, M.T., 1982. Effect of temperature and salinity on Vibrio (Beneckea) vulnificus occurrence in a Gulf Coast environment. *Applied and Environmental Microbiology*, *44*(4), pp.820-824.

Kim, C.K. and Park, K., 2012. A modeling study of water and salt exchange for a micro-tidal, stratified northern Gulf of Mexico estuary. *Journal of Marine Systems*, *96*, pp.103-115.

Kim, C.K., Park, K. and Powers, S.P., 2013. Establishing restoration strategy of eastern oyster via a coupled biophysical transport model. *Restoration Ecology*, *21*(3), pp.353-362.

Kinsey, T.P., Lydon, K.A., Bowers, J.C. and Jones, J.L., 2015. Effects of dry storage and resubmersion of oysters on total Vibrio vulnificus and total and pathogenic (tdh+/trh+) Vibrio parahaemolyticus levels. *Journal of food protection*, *78*(8), pp.1574-1580.

Koga, T., Katagiri, T., Hori, H. and Takumi, K., 2002. Alkaline adaptation induces cross-protection against some environmental stresses and morphological change in Vibrio parahaemolyticus. *Microbiological Research*, *157*(4), pp.249-255.

Krause, J. W., Brzezinski, M. A., Largier, J. L., McNair, H. M., Maniscalco, M., Bidle, K. D., & Thamatrakoln, K., 2020. The interaction of physical and biological factors drives phytoplankton spatial distribution in the northern California Current. *Limnology and Oceanography*, *65*(9), pp.1974-1989.

Landsberg, J.H., 2002. The effects of harmful algal blooms on aquatic organisms. *Reviews in Fisheries Science*, *10*(2), pp.113-390.

Lee, J., Webb, B.M., Dzwonkowski, B., Valle-Levinson, A. and Lee, J., 2019. Characteristics of exchange flow in a multiple inlet diurnal estuary: Mobile Bay, Alabama. *Journal of Marine Systems*, *191*, pp.38-50.

Lehrter, J.C., Pennock, J.R. and McManus, G.B., 1999. Microzooplankton grazing and nitrogen excretion across a surface estuarine-coastal interface. *Estuaries*, *22*(1), pp.113-125.

Liefer, J. D., Robertson, A., MacIntyre, H.L., Smith, W.L., and Dorsey, C.P., 2013. Characterization of a toxic Pseudo-nitzschia spp. bloom in the Northern Gulf of Mexico associated with domoic acid accumulation in fish. *Harmful Algae*. 26, pp. 20-32.

Lipp, E.K., Rodriguez-Palacios, C. and Rose, J.B., 2001. Occurrence and distribution of the human pathogen Vibrio vulnificus in a subtropical Gulf of Mexico estuary. *The Ecology and Etiology of Newly Emerging Marine Diseases*. pp. 165-173.

Macintyre, H. L., Stutes, A. L., Smith, W. L., Dorsey, C. P., Abraham, A., & Dickey, R. W., 2011. Environmental correlates of community composition and toxicity during a bloom of Pseudo-nitzschia spp. in the northern Gulf of Mexico. *Journal of Plankton Research*, *33*(2), 273-295.

Main, C.R., Salvitti, L.R., Whereat, E.B. and Coyne, K.J., 2015. Community-level and species-specific associations between phytoplankton and particle-associated Vibrio species in Delaware's inland bays. *Applied and Environmental Microbiology*, *81*(17), pp.5703-5713.

McCarter, L.L., 2001. Polar flagellar motility of the Vibrionaceae. *Microbiology and Molecular Biology Reviews*, *65*(3), pp.445-462.

Mississippi Department of Marine Resources, 2019. Blue-Green Algal Bloom FAQ. Accessed from: https://dmr.ms.gov/algal-blooms/.

Mobile Bay National Estuary Program. 2019. The Coast. Accessed from: http://www.mobilebaynep.com/the_landscape/the_alabama_coast/

Montanari, M.P., Pruzzo, C., Pane, L. and Colwell, R.R., 1999. Vibrios associated with plankton in a coastal zone of the Adriatic Sea (Italy). *FEMS Microbiology Ecology*, *29*(3), pp.241-247

.

Moran, M.A., 2015. The global ocean microbiome. *Science*, *350*(6266).

Morris, J.J., Lenski, R.E. and Zinser, E.R., 2012. The Black Queen Hypothesis: evolution of dependencies through adaptive gene loss. *MBio*, *3*(2), pp. e00036-12.

Motes, M.L., DePaola, A., Cook, D.W., Veazey, J.E., Hunsucker, J.C., Garthright, W.E., Blodgett, R.J. and Chirtel, S.J., 1998. Influence of water temperature and salinity on Vibrio vulnificus in Northern Gulf and Atlantic Coast oysters (Crassostrea virginica). *Applied and Environmental Microbiology*, *64*(4), pp.1459-1465.

Nash, J.E., 2018. *Vibrio cholerae Abundance in Mobile Bay, AL* (Master's thesis, University of South Alabama).

NOAA Fisheries. 2020. *2019 Bottlenose Dolphin Unusual Mortality Event Along the Northern Gulf of Mexico*. National Oceanic and Atmospheric Administration - Fisheries. https://www.fisheries.noaa.gov/national/marine-life-distress/2019-bottlenose-dolphin-unusual-mortality-event-along-northern-gulf.

Nordstrom, J.L., Vickery, M.C., Blackstone, G.M., Murray, S.L. and DePaola, A., 2007. Development of a multiplex real-time PCR assay with an internal amplification control for the detection of total and pathogenic Vibrio parahaemolyticus bacteria in oysters. *Applied and Environmental Microbiology*, *73*(18), pp.5840-5847.

Percival, S.L. and Williams, D.W., 2014. Vibrio. Academic Press. *Microbiology of Waterborne Diseases,* (pp. 237-248).

Pruzzo, C., Huq, A., Colwell, R.R. and Donelli, G., 2005. Pathogenic Vibrio species in the marine and estuarine environment. *Oceans and Health: Pathogens in the Marine Environment* (pp. 217-252).

Randa, M.A., Polz, M.F. and Lim, E., 2004. Effects of temperature and salinity on Vibrio vulnificus population dynamics as assessed by quantitative PCR. *Applied and Environmental Microbiology*, *70*(9), pp.5469-5476.

Rehnstam-Holm, A.S., Godhe, A., Härnström, K., Raghunath, P., Saravanan, V., Collin, B., Karunasagar, I. and Karunasagar, I., 2010. Association between phytoplankton and Vibrio spp. along the southwest coast of India: a mesocosm experiment. *Aquatic Microbial Ecology*, *58*(2), pp.127-139.

Schlitzer, R., 2021. Ocean Data View, https://odv.awi.de.

Schroeder, W.W. and Wiseman Jr, W.J., 1986. Low-frequency shelf-estuarine exchange processes in Mobile Bay and other estuarine systems on the northern Gulf of Mexico. Academic Press. *Estuarine Variability,* pp. 355-367.

Schroeder, W.W., Wiseman, W.J., Bianchi, T.S., Pennock, J.R. and Twilley, R.R., 1999. Geology and hydrodynamics of Gulf of Mexico estuaries. *Biogeochemistry of Gulf of Mexico Estuaries*, pp.3-28.

Siboni, N., Balaraju, V., Carney, R., Labbate, M. and Seymour, J.R., 2016. Spatiotemporal dynamics of Vibrio spp. within the Sydney Harbour estuary. *Frontiers in Microbiology*, *7*, pp.460.

Steidinger, K. A., and H. L. Penta (eds.). 1999. Harmful microalgae and associated public health risks in the Gulf of Mexico. Report for the U.S. EPA Gulf of Mexico Program by the Florida Department of Environmental Protection, Florida Marine Research Institute, St.Petersburg. http://research.myfwc.com/publications/publication_info.asp?id=39879. Accessed September 17, 2019

Takemura, A.F., Chien, D.M. and Polz, M.F., 2014. Associations and dynamics of Vibrionaceae in the environment, from the genus to the population level. *Frontiers in Microbiology*, *5*, p.38.

Turner, J.W., Good, B., Cole, D. and Lipp, E.K., 2009. Plankton composition and environmental factors contribute to Vibrio seasonality. *The ISME Journal*, *3*(9), pp.1082-1092.

Urquhart, E.A., Jones, S.H., Yu, J.W., Schuster, B.M., Marcinkiewicz, A.L., Whistler, C.A. and Cooper, V.S., 2016. Environmental conditions associated with elevated Vibrio parahaemolyticus concentrations in Great Bay Estuary, New Hampshire. *PloS one*, *11*(5), pp. e0155018.

Vanoy, R.W., Tamplin, M.L. and Schwarz, J.R., 1992. Ecology of Vibrio vulnificus in Galveston Bay oysters, suspended particulate matter, sediment and seawater: detection by monoclonal antibody—immunoassay—most probable number procedures. *Journal of Industrial Microbiology and Biotechnology*, *9*(3-4), pp.219-223.

Williams, L.A. and LaRock, P.A., 1985. Temporal occurrence of Vibrio species and Aeromonas hydrophila in estuarine sediments. *Applied and Environmental Microbiology*, *50*(6), pp.1490-1495.

Wright, A.C., Hill, R.T., Johnson, J.A., Roghman, M.C., Colwell, R.R. and Morris Jr, J.G., 1996. Distribution of Vibrio vulnificus in the Chesapeake Bay. *Applied and Environmental Microbiology*, *62*(2), pp.717-724.

Yildiz, F.H. and Visick, K.L., 2009. Vibrio biofilms: so much the same yet so different. *Trends in Microbiology*, *17*(3), pp.109-118.

Zimmerman, A.M., DePaola, A., Bowers, J.C., Krantz, J.A., Nordstrom, J.L., Johnson, C.N. and Grimes, D.J., 2007. Variability of total and pathogenic Vibrio parahaemolyticus densities in northern Gulf of Mexico water and oysters. *Applied and Environmental Microbiology*, *73*(23), pp.7589-7596.

BIOGRAPHICAL SKETCH

Name of Author: Blair H. Morrison

Graduate and Undergraduate Schools Attended:
2019-2021 - University of South Alabama
2014-2018 – The University of Alabama

Degrees Awarded:
Master of Science. Marine Sciences – University of South Alabama
Bachelor of Science. Marine Science and Biology – The University of Alabama

Awards and Honors:
2021 National Academy of Sciences – Gulf Research Program Science Policy Fellow
2019-2021 FDA/DISL Research Fellow – University of South Alabama
2016 NOAA Ernest F. Hollings Scholar – The University of Alabama

Publications:

Denise D Colombano, Steven Y Litvin, Shelby L Ziegler, Scott B Alford, Ronald Baker, Myriam A Barbeau, Just Cebrián, Rod M Connolly, Carolyn A Currin, Linda A Deegan, Justin S Lesser, Charles W Martin, Ashley E McDonald, Catherine McLuckie, **Blair H Morrison**, James W Pahl, L Mark Risse, Joseph AM Smith, Lorie W Staver, R Eugene Turner, Nathan J Waltham. 2021. Climate change implications for tidal marshes and food web linkages to estuarine and coastal nekton. *Estuaries and Coasts*, pp.1-12.

Ronald Baker, Matthew D Taylor, Kenneth W Able, Michael W Beck, Just Cebrian, Denise D Colombano, Rod M Connolly, Carolyn Currin, Linda A Deegan, Ilka C Feller, Ben L Gilby, Matthew E Kimball, Thomas J Minello, Lawrence P Rozas, Charles Simenstad, R Eugene Turner, Nathan J Waltham, Michael P Weinstein, Shelby L Ziegler, Philine SE Zu Ermgassen, Caitlin Alcott, Scott B Alford, Myriam A Barbeau, Sarah C Crosby, Kate Dodds, Alyssa Frank, Janelle Goeke, Lucy A Goodridge Gaines, Felicity E Hardcastle, Christopher J Henderson, W Ryan James, Matthew D Kenworthy, Justin Lesser, Debbrota Mallick, Charles W Martin, Ashley E McDonald, Catherine McLuckie,

Blair H Morrison, James A Nelson, Gregory S Norris, Jeff Ollerhead, James W Pahl, Sarah Ramsden, Jennifer S Rehage, James F Reinhardt, Ryan J Rezek, L Mark Risse, Joseph AM Smith, Eric L Sparks, Lorie W Staver. 2020. Fisheries rely on threatened salt marshes. *Science*, *370*(6517), pp.670-671.

Ben L Gilby, Michael P Weinstein, Ronald Baker, Just Cebrian, Scott B Alford, Ariella Chelsky, Denise Colombano, Rod M Connolly, Carolyn A Currin, Ilka C Feller, Alyssa Frank, Janelle A Goeke, Lucy A Goodridge Gaines, Felicity E Hardcastle, Christopher J Henderson, Charles W Martin, Ashley E McDonald, **Blair H Morrison**, Andrew D Olds, Jennifer S Rehage, Nathan J Waltham, Shelby L Ziegler. 2020. Human actions alter tidal marsh seascapes and the provision of ecosystem services. *Estuaries and Coasts*, pp.1-9.